Electronic Supplementary Material (ESI) for Green Chemistry.

Electronic Supplementary Information for

Isotruxene-Based Porous Polymers as Efficient and Recyclable Photocatalysts for Visible-Light-Induced Metal-Free Oxidative Organic Transformations

Haowen Zhang,[a] Cen Zhou,*[b] Ying Zheng,[a] and Xiao Zhang*[a]

[a]Fujian Key Laboratory of Polymer Materials, Fujian Provincial Key Laboratory of Advanced Materials Oriented Chemical Engineering, College of Chemistry and Materials Science, Fujian Normal University, 8 Shangsan Lu, Fuzhou 350007, China

E-mail: zhangxiao@fjnu.edu.cn

[b]Fujian Engineering and Research Center of New Chinese Lacquer Materials, Ocean College, Minjiang University, Fuzhou 350108, China

E-mail: zhoucen@mju.edu.cn

Table of Contents

1. General Information S3

2. Synthesis S4

3. Characterization of IsoPOP-1 and IsoPOP-2 .... S6

4. General Procedure for Visible-Light-Induced Oxidative Hydroxylation of Arylboronic Acids S13

5. General Procedure for Visible-Light-Induced Oxidation of Aldehydes S18

6. Recyclability Tests of IsoPOP-1 and IsoPOP-2 .... S23

7. Mechanistic Studies S25

8. Comparision with Known Photocatalysts S27

9. References S29

10. Copies of NMR Spectra S31

1. General Information

Unless stated otherwise, all reactions were carried out in flame-dried glassware under a dry nitrogen atmosphere. All reagents were commercially purchased and used without any further purification. ^1H spectra were recorded on a Bruker instrument (400 MHz) and internally referenced to tetramethylsilane signal or residual protic solvent signals. Data for ^1H NMR are recorded as follows: chemical shift (δ, ppm), multiplicity (s = singlet, d = doublet, t = triplet, m = multiplet or unresolved, br = broad singlet, coupling constant(s) in Hz, integration).

Powder X-ray diffraction (PXRD) was recorded on a PANalytical X'pert PRO X-ray Diffractometer using Cu-Kα radiation in the 2θ range of 10-90°. The nitrogen adsorption-desorption isotherms at 77 K were measured with a Micromeritics ASAP2460 analyzers, and the BET surface area was estimated by the Brunauer-Emmett-Teller (BET) theory. Fourier Transform Infrared spectra were recorded with a Nicolet iS50 FT-IR spectrophotometer. UV-vis diffuse reflectance spectra (DRS) were performed on a Perkin Elmer Lambda 750 in the 300~800 nm range, with $BaSO_4$ as the reference substance. Electrochemical measurements were performed on an electrochemical workstation (CHI 660E, CH Instruments Inc., Shanghai). Thermogravimetric analysis (TGA) profiles were recorded on a METTLER TGA/SDTA 851 thermal analyzer. Scanning electron microscopy (SEM) images were recorded using a Phenomenon LE electron microscope. Electron Spin Resonance (ESR) spectra were collected on a Bruker EMX instrument. HOMO-LUMO energy levels were calculated with Gaussian 09 using the density function theory RB3LYP/6311G method.

Emission spectra of the LED lamps

The following spectra were recorded on EVERFINE Corporation HAAS-2000_VIS_V2 High-precision fast spectroradiometer. The forward current of the LEDs is 25 mA. Electroluminescence (EL) measurements of the LED lamps were carried out at room temperature using Everfine HAAS-2000. For the light collection, the LEDs were placed inside a 30 cm-diameter integrating sphere coupled to a high accuracy array spectroradiometer (wavelength accuracy <0.3 nm) and a programmable test power LED300E.

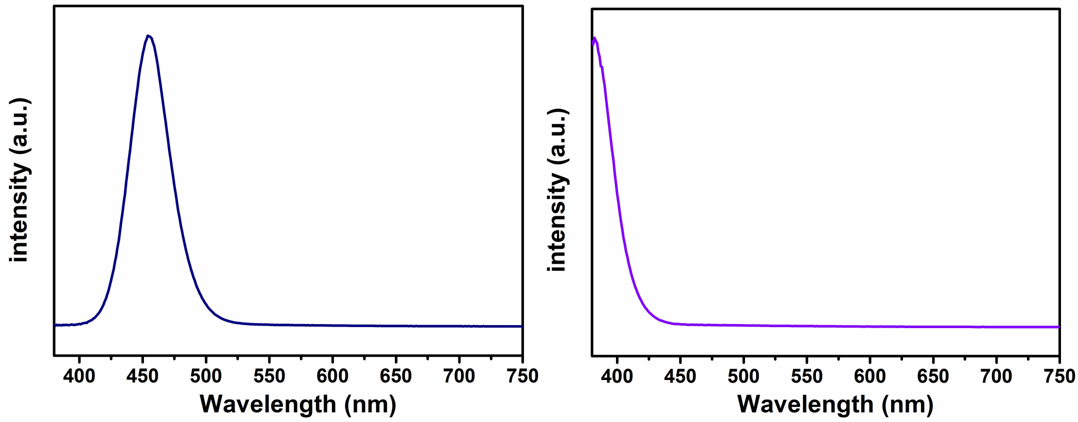

Figure S1 Emission spectra of the blue LEDs lamp (left) and the purple LEDs lamp (right).

2. Synthesis

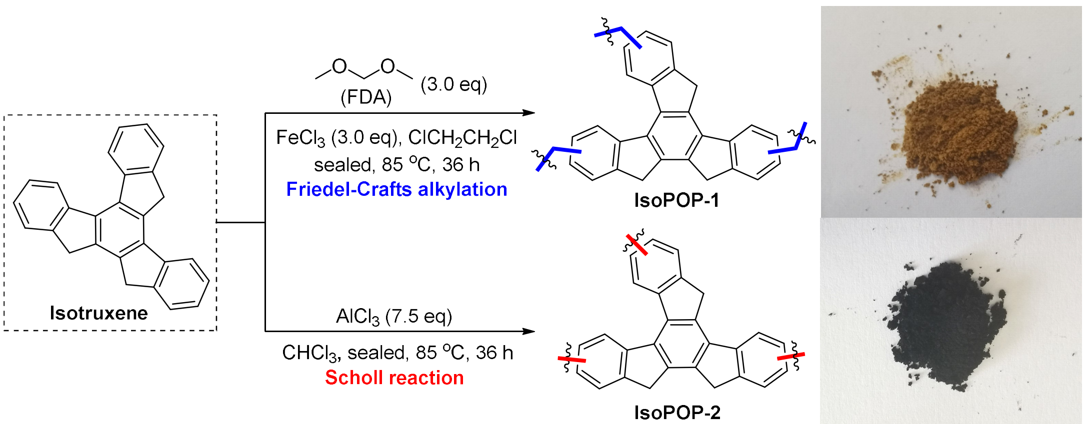

Synthesis of IsoPOP-1:

$FeCl_3$ (2.13 g, 13.14 mmol, anhydrous) was added to a solution of isotruxene (1.5 g, 4.38 mmol) in 20 mL 1, 2-dichloroethane (DCE). After being stirred at room temperature for 15 min, dimethoxymethane (1.16 mL, 13.14 mmol) was added. Then the resulting mixture was stirred at 85 °C for 36 h to complete the cross-linking. Afterwards, the reaction mixture was cooled to room temperature and the obtained precipitate was washed with water, acetone, ethanol, ethyl acetate, dichloromethane and petroleum ether, respectively. The product IsoPOP-1 was collected and dried under vacuum as brown powders (1.29 g, 69% yield).

Synthesis of IsoPOP-2:

$AlCl_3$ (4.38 g, 32.85 mmol, anhydrous) was added to a solution of isotruxene (1.5 g, 4.38 mmol) in 15 mL trichloromethane. Then the resulting mixture was stirred at 85 °C for 36 h to complete the cross-linking. Afterwards, the reaction mixture was cooled to room temperature and the obtained precipitate was washed with water, acetone, ethanol, ethyl acetate, dichloromethane and petroleum ether, respectively. The product IsoPOP-2 was collected and dried under vacuum as black powders (1.42 g, 85% yield).

3. Characterization of IsoPOP-1 and IsoPOP-2

Surface Area	
Single point surface area at P/Po = 0.275153590:	734.7572 m²/g
BET Surface Area:	727.3466 m²/g
t-Plot Micropore Area:	586.2145 m²/g
t-Plot external surface area:	507.1241 m²/g
Pore Volume	
Single point adsorption total pore volume of pores less than 40.3122 nm width at P/Po = 0.950000000:	0.813562 cm³/g
Single point desorption total pore volume of pores less than 40.3122 nm width at P/Po = 0.950000000:	0.809324 cm³/g
BJH Adsorption cumulative volume of pores between 1.7000 nm and 300.0000 nm width:	0.831256 cm³/g
BJH Desorption cumulative volume of pores between 1.7000 nm and 300.0000 nm width:	0.828652cm³/g
Pore Size	
BJH Adsorption average pore width (4V/A):	0.514586 nm
BJH Desorption average pore width (4V/A):	0.512345 nm

Surface Area	
Single point surface area at P/Po = 0.275153590:	556.8967 m²/g
BET Surface Area:	543.1782 m²/g
t-Plot Micropore Area:	379.5679 m²/g
t-Plot external surface area:	327.2589 m²/g
Pore Volume	
Single point adsorption total pore volume of pores less than 40.3122 nm width at P/Po = 0.950000000:	0.815676 cm³/g
Single point desorption total pore volume of pores less than 40.3122 nm width at P/Po = 0.950000000:	0.819852 cm³/g
BJH Adsorption cumulative volume of pores between 1.7000 nm and 300.0000 nm width:	0.821352 cm³/g
BJH Desorption cumulative volume of pores between 1.7000 nm and 300.0000 nm width:	0.822325 cm³/g
Pore Size	
BJH Adsorption average pore width (4V/A):	0.542765 nm
BJH Desorption average pore width (4V/A):	0.537683 nm

Fig. S2 Pore properties of IsoPOP-1 (left) and IsoPOP-2 (right).

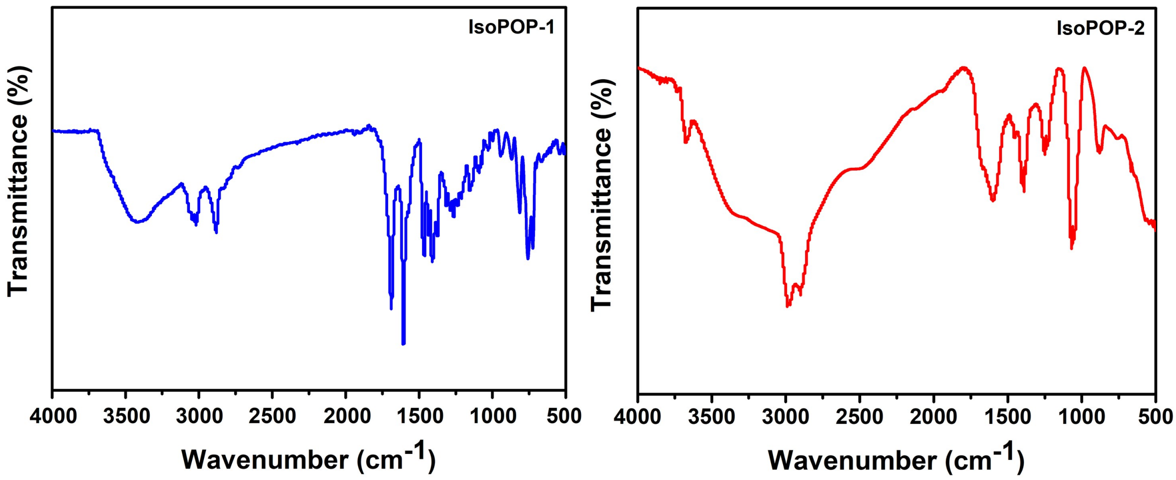

Fig. S3 FTIR spectra of IsoPOP-1 and IsoPOP-2.

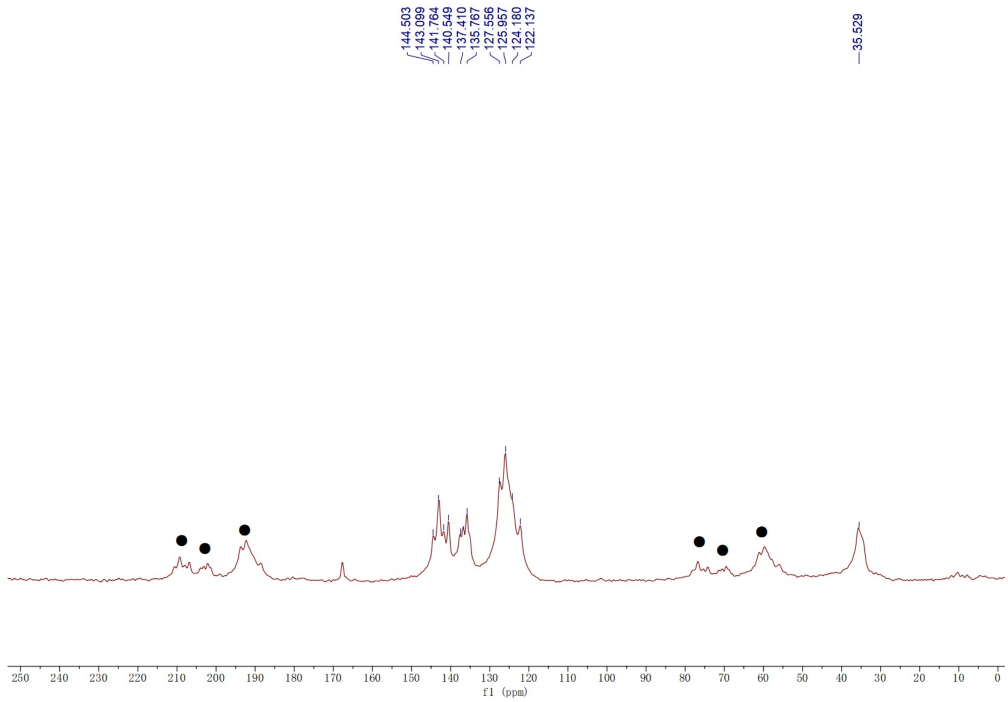

Fig. S4 Solid-state ^{13}C CP/MAS NMR (600 MHz) spectra of IsoPOP-1.

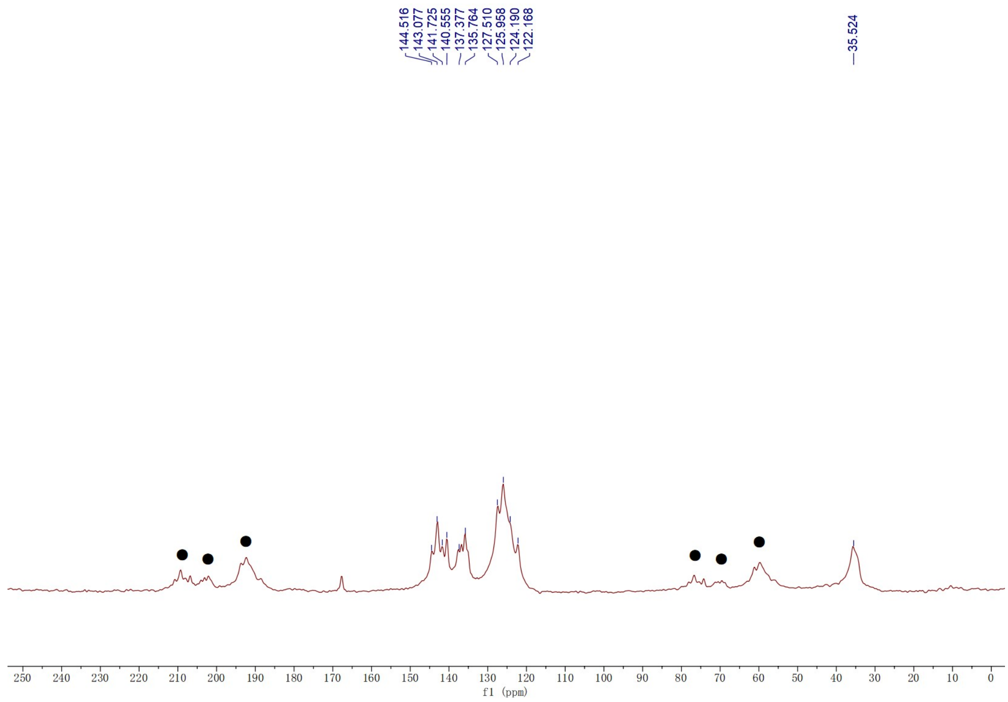

Fig. S5 Solid-state ^{13}C CP/MAS NMR (600 MHz) spectra of IsoPOP-2.

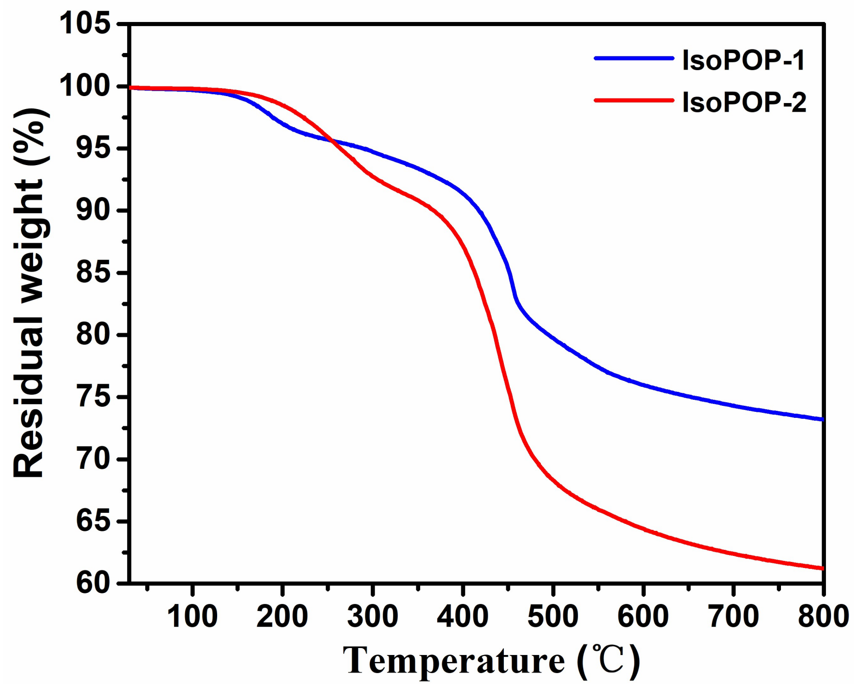

Fig. S6 TGA spectra of IsoPOP-1 and IsoPOP-2.

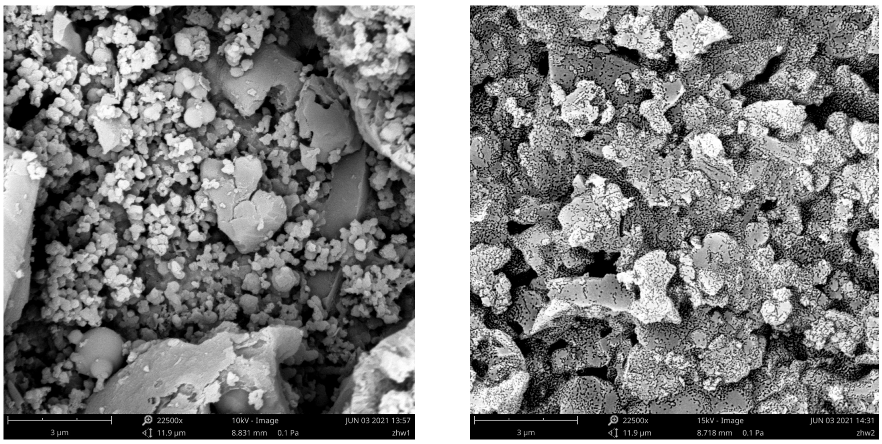

Fig. S7 SEM images of IsoPOP-1 and IsoPOP-2.

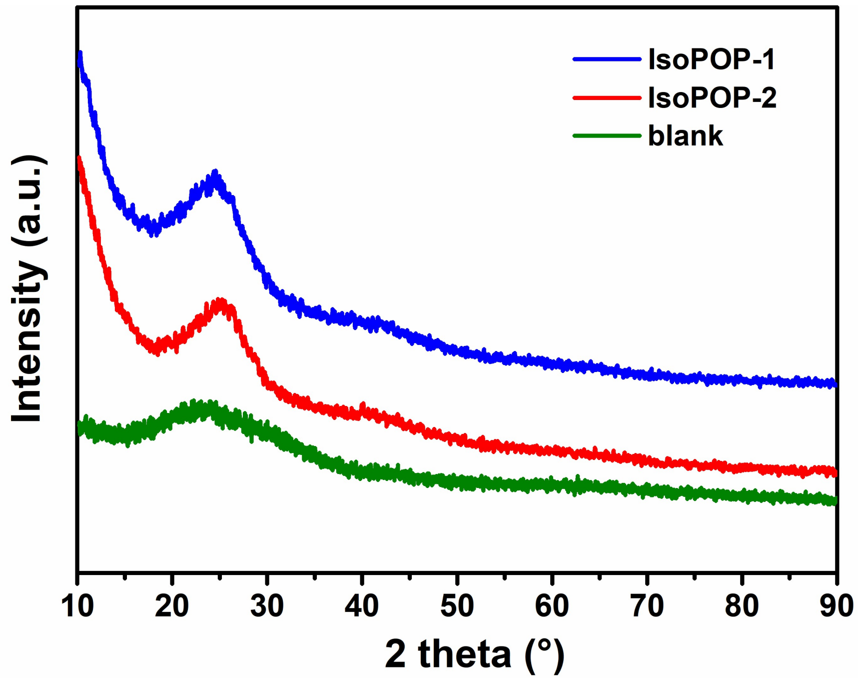

Fig. S8 PXRD patterns of IsoPOP-1 and IsoPOP-2.

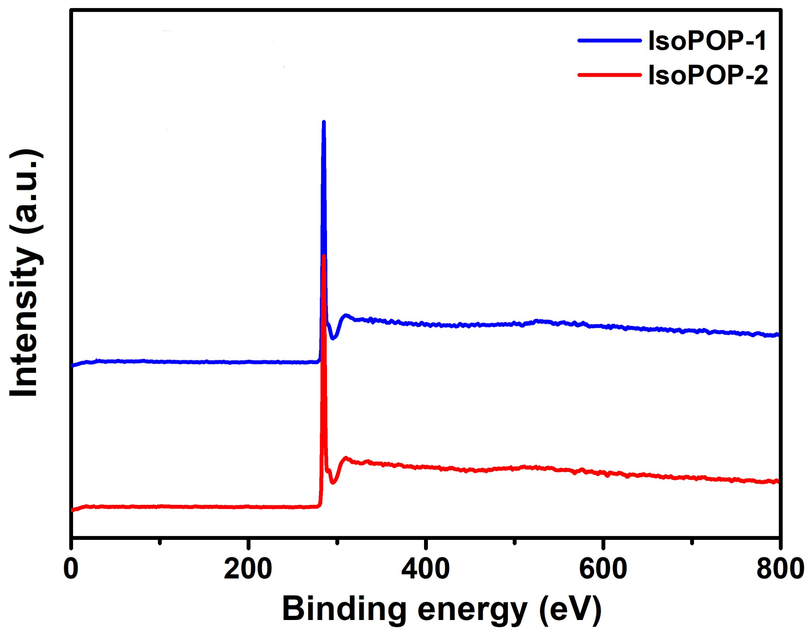

Fig. S9 XPS survey scan of IsoPOP-1 and IsoPOP-2.

Table S1 Elemental analysis of IsoPOP-1 and IsoPOP-2.

Material	Exp. (%)				
	C	H	N	S	O
IsoPOP-1 (Calculated for $C_{33}H_{30}$ as repeat unit)	92.83	7.03	-	-	0.00
IsoPOP-1	92.77	5.32	-	-	0.00
IsoPOP-2 (Calculated for $C_{30}H_{24}$ as repeat unit)	93.62	6.24	-	-	0.00
IsoPOP-2	95.12	3.87	-	-	0.00

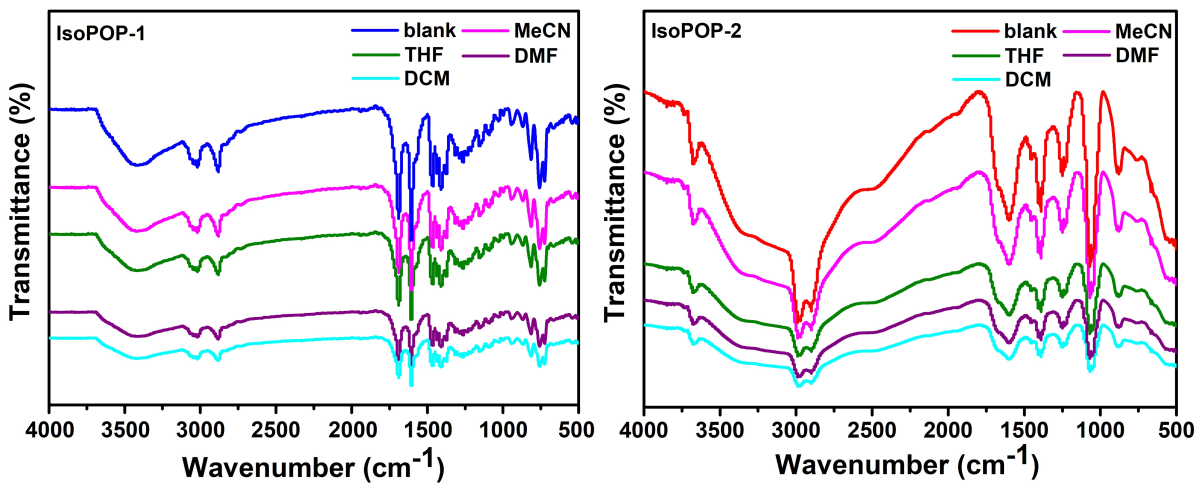

Fig. S10 FTIR spectra of IsoPOP-1 and IsoPOP-2 treated with different solvents (continuous ultrasound for 2h).

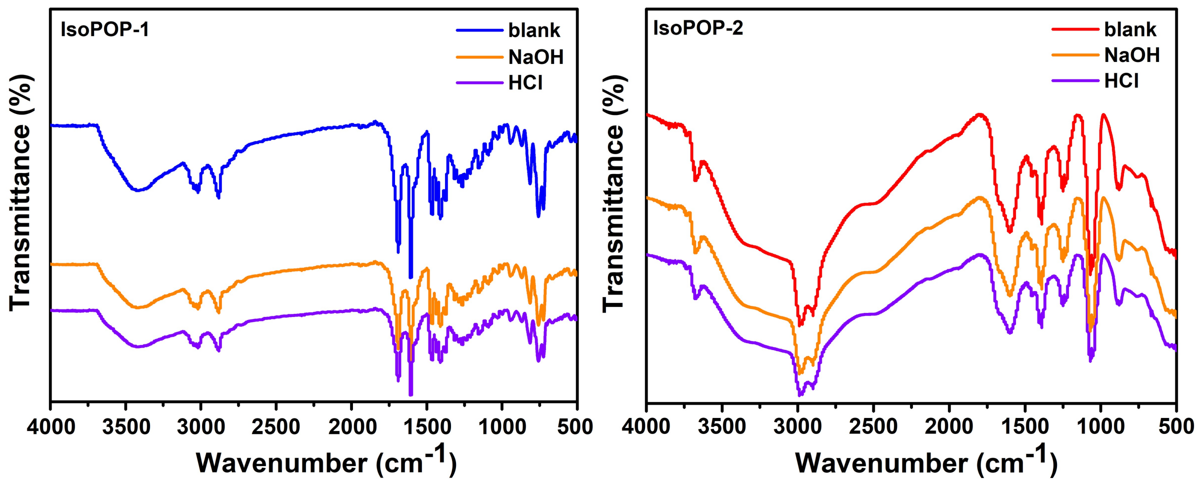

Fig. S11 FTIR spectra of IsoPOP-1 and IsoPOP-2 treated with NaOH (pH = 13) and HCl (pH =1) (continuous ultrasound for 2h).

Table S2 DFT calculated HOMO-LUMO energy levels for IsoPOP-1 and IsoPOP-2.

Polymer	HOMO (eV)	LUMO (eV)	Band gap (eV)
IsoPOP-1	-0.18796	-0.04112	0.14684
IsoPOP-2	-0.18755	-0.04061	0.14694

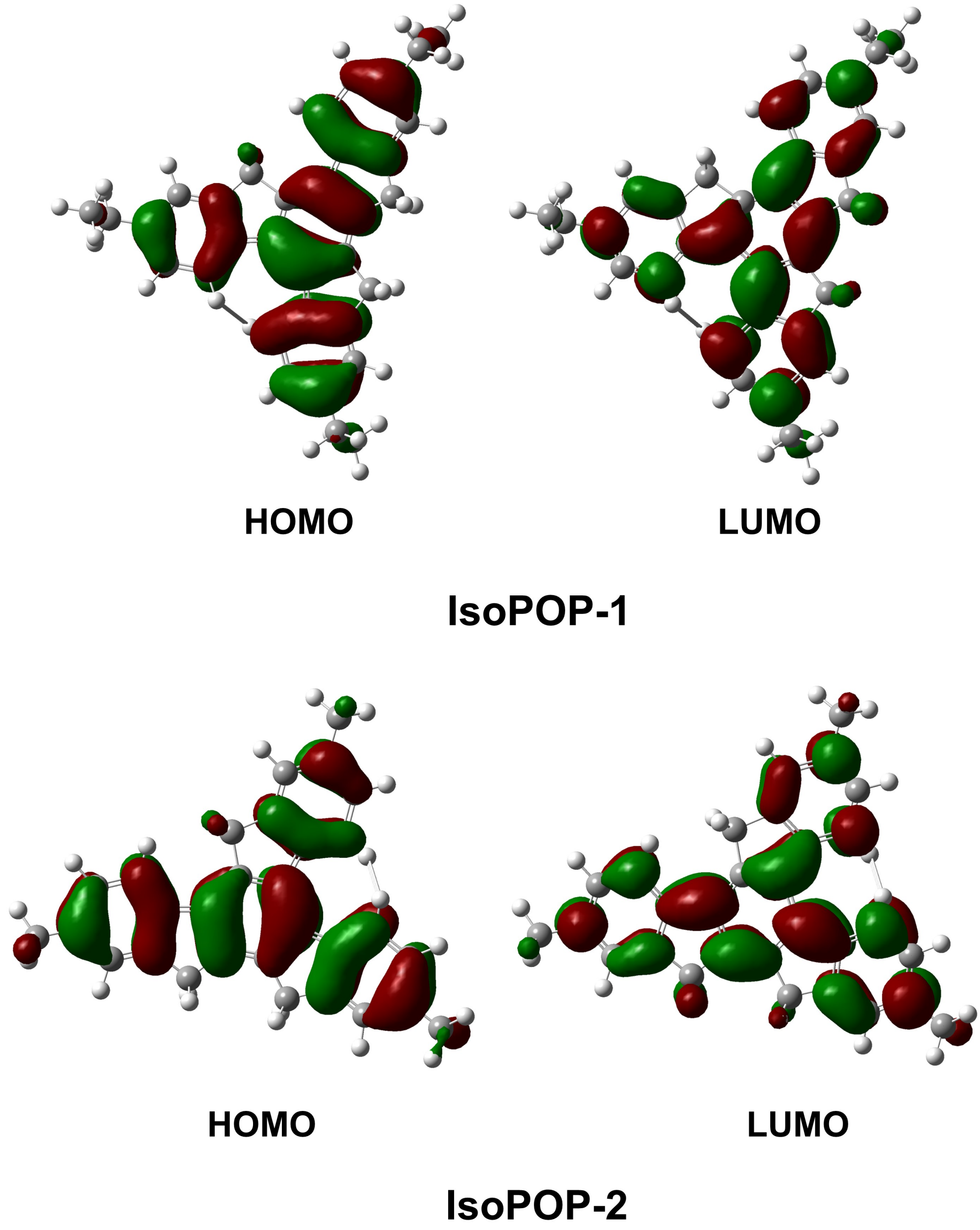

Fig. S12 HOMO-LUMO band structures of IsoPOP-1 and IsoPOP-2 repeating units.

4. General Procedure for Visible-Light-Induced Oxidative Hydroxylation of Arylboronic Acids

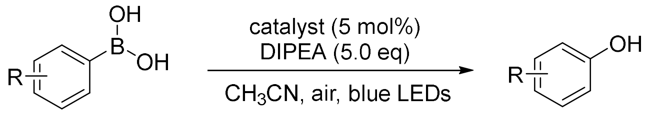

1 **2**

To a Schlenk tube were added the substrate **1** (0.2 mmol, 1.0 equiv), DIPEA (1 mmol, 5.0 equiv), IsoPOP-1 or IsoPOP-2 (5 mol%), and acetonitrile (2 mL). The reaction mixture was positioned approximately 2~3 cm from a 30 W blue LEDs lamp under air. The mixture was stirred at room temperature for the indicated time (monitored by TLC). Afterwards, the catalyst was separated by microcentrifuge and washed with dichloromethane. Then the filtrate was concentrated by rotary evaporation and the residue was purified by silica gel flash column chromatography using ethyl acetate/petroleum ether as the eluent to afford the desired products **2**. The analytical data of the products are summarized below.

Table S3 Optimization of the amounts of DIPEA.

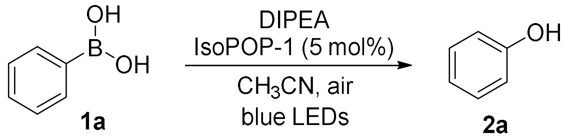

1a **2a**

Entry	DIPEA (eq)	Time (h)	Yield (%)
1	1.0	18	67
2	2.0	7.0	82
3	3.0	3.0	90
4	4.0	1.5	99
5	5.0	1.0	99

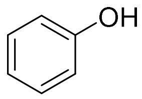

2a

2a,[1] white solid, IsoPOP-1: 18.6 mg, 99% yield; IsoPOP-2: 18.6 mg, 99% yield. ^{1}H NMR (400 MHz, $CDCl_3$): δ 7.24 (t, *J* = 8.4 Hz, 2H), 6.93 (t, *J* = 7.6 Hz, 1H), 6.83 (d, *J* = 8.8 Hz, 2H), 5.29 (s, 1H).

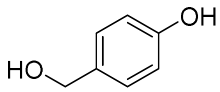

2b

2b,[2] white solid, IsoPOP-1: 24.3 mg, 98% yield; IsoPOP-2: 24.1 mg, 97% yield. ^{1}H NMR (400 MHz, DMSO-d_6): δ 9.23 (s, 1H), 7.10 (d, *J* = 8.4 Hz, 2H), 6.70 (d, *J* = 8.4 Hz, 2H), 4.95 (t, *J* = 5.6 Hz, 1H), 4.35 (d, *J* = 5.6 Hz, 2H).

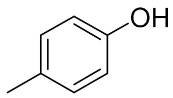

2c

2c,[1] white solid, IsoPOP-1: 21.4 mg, 99% yield; IsoPOP-2: 21.2 mg, 98% yield. ^{1}H NMR (400 MHz, $CDCl_3$): δ 7.02 (d, *J* = 8.0 Hz, 2H), 6.73 (d, *J* = 8.4 Hz, 2H), 5.37 (br, 1H), 2.26 (s, 3H).

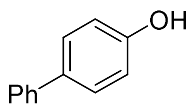

2d

2d,[1] white solid, IsoPOP-1: 33.7 mg, 99% yield; IsoPOP-2: 33.0 mg, 97% yield. ^{1}H NMR (400 MHz, DMSO-d_6): δ 9.56 (s, 1H), 7.57 (d, *J* = 7.2 Hz, 2H), 7.49 (d, *J* = 8.8 Hz, 2H), 7.40 (t, *J* = 7.6 Hz, 2H), 7.27 (t, *J* = 7.2 Hz, 1H), 6.86 (d, *J* = 8.4 Hz, 2H).

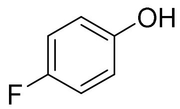

2e

2e,[1] white solid, IsoPOP-1: 20.6 mg, 92% yield; IsoPOP-2: 20.0 mg, 89% yield. ^{1}H NMR (400 MHz, $CDCl_3$): δ 6.95-6.90 (m, 2H), 6.79-6.75 (m, 2H), 4.95 (s, 1H).

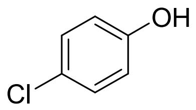

2f

2f,[1] white solid, IsoPOP-1: 24.9 mg, 97% yield; IsoPOP-2: 24.2 mg, 94% yield. ^{1}H NMR (400 MHz, $CDCl_3$): δ 7.21-7.17 (m, 2H), 6.78-6.75 (m, 2H), 5.08-5.01 (m, 1H).

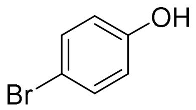

2g

2g,[2] white solid, IsoPOP-1: 31.8 mg, 92% yield; IsoPOP-2: 31.5 mg, 91% yield. ^{1}H NMR (400 MHz, $CDCl_3$): δ 7.33 (d, J = 9.2 Hz, 2H), 6.72 (d, J = 9.2 Hz, 2H), 5.11 (br, 1H).

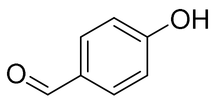

2h

2h,[1] white solid, IsoPOP-1: 24.2 mg, 99% yield; IsoPOP-2: 23.9 mg, 98% yield. ^{1}H NMR (400 MHz, $CDCl_3$): δ 9.86 (s, 1H), 7.82 (d, J = 8.8 Hz, 2H), 6.99 (d, J = 8.4 Hz, 2H), 6.85 (s, 1H).

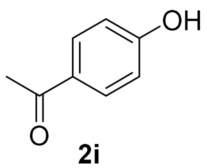

2i

2i,[3] white solid, IsoPOP-1: 25.9 mg, 95% yield; IsoPOP-2: 24.8 mg, 91% yield. ^{1}H NMR (400 MHz, $CDCl_3$): δ 7.92 (d, J = 8.4 Hz, 2H), 6.92 (d, J = 8.4 Hz, 2H), 6.58 (s, 1H), 2.58 (s, 3H).

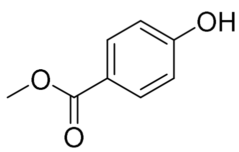

2j

2j,[3] white solid, IsoPOP-1: 29.5 mg, 97% yield; IsoPOP-2: 28.9 mg, 95% yield. ^{1}H NMR (400 MHz, DMSO-d_6): δ 10.36 (br, 1H), 7.82 (d, J = 8.8 Hz, 2H), 6.86 (d, J = 8.8 Hz, 2H), 3.79 (s, 3H).

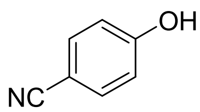

2k

2k,[1] white solid, IsoPOP-1: 22.6 mg, 95% yield; IsoPOP-2: 21.7 mg, 91% yield. ^{1}H NMR (400 MHz, $CDCl_3$): δ 7.55 (d, J = 8.8 Hz, 2H), 6.93 (d, J = 8.8 Hz, 2H), 6.65 (br, 1H).

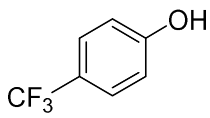

2l

2l,[1] white solid, IsoPOP-1: 30.2 mg, 93% yield; IsoPOP-2: 29.2 mg, 90% yield. ^{1}H NMR (400 MHz, $CDCl_3$): δ 7.51 (d, J = 8.0 Hz, 2H), 6.90 (d, J = 8.0 Hz, 2H), 5.46 (s, 1H).

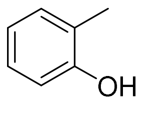

2m

2m,[1] white solid, IsoPOP-1: 21.4 mg, 99% yield; IsoPOP-2: 20.5 mg, 95% yield. ^{1}H NMR (400 MHz, $CDCl_3$): δ 7.13-7.07 (m, 2H), 6.85 (t, J = 7.2 Hz, 1H), 6.77 (d, J = 9.2 Hz, 1H), 4.78 (s, 1H), 2.26 (s, 3H).

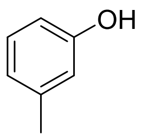

2n

2n,[1] white solid, IsoPOP-1: 21.4 mg, 99% yield; IsoPOP-2: 21.0 mg, 97% yield. ^{1}H NMR (400 MHz, $CDCl_3$): δ 7.12 (t, *J* = 7.6 Hz, 1H), 6.75 (d, *J* = 7.6 Hz, 1H), 6.65-6.63 (m, 2H), 4.98 (br, 1H), 2.30 (s, 3H).

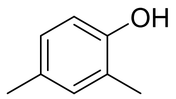

2o

2o,[3] white solid, IsoPOP-1: 23.9 mg, 98% yield; IsoPOP-2: 23.3 mg, 95% yield. ^{1}H NMR (400 MHz, $CDCl_3$): δ 6.98 (d, *J* = 7.6 Hz, 2H), 6.76 (t, *J* = 7.6 Hz, 1H), 4.60 (s, 1H), 2.25 (s, 6H).

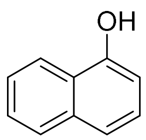

2p

2p,[3] purple solid, IsoPOP-1: 26.8 mg, 93% yield; IsoPOP-2: 26.2 mg, 91% yield. ^{1}H NMR (400 MHz, $CDCl_3$): δ 8.19-8.17 (m, 1H), 7.83-7.80 (m, 1H), 7.50-7.43 (m, 3H), 7.30 (t, *J* = 7.6 Hz, 1H), 6.82 (d, *J* = 7.2 Hz, 1H), 5.34 (s, 1H).

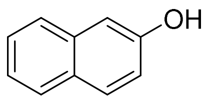

2q

2q,[1] white solid, IsoPOP-1: 27.4 mg, 95% yield; IsoPOP-2: 26.5 mg, 92% yield. ^{1}H NMR (400 MHz, $CDCl_3$): δ 7.78-7.74 (m, 2H), 7.67 (d, *J* = 8.4 Hz, 1H), 7.44-7.40 (m, 1H), 7.34-7.30 (m, 1H), 7.14 (d, *J* = 2.4 Hz, 1H), 7.10 (dd, *J* = 8.8, 2.8 Hz, 1H), 5.16 (s, 1H).

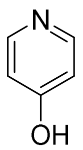

2r

2r,[3] white solid, IsoPOP-1: 17.7 mg, 93% yield; IsoPOP-2: 17.1 mg, 90% yield. ^{1}H NMR (400 MHz, DMSO-d_6): δ 11.26 (br, 1H), 7.69 (d, J = 6.8 Hz, 2H), 6.16 (d, J = 6.8 Hz, 2H).

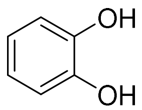

2s

2s,[4] white solid, IsoPOP-1: 18.7 mg, 85% yield; IsoPOP-2: 17.6 mg, 80% yield. ^{1}H NMR (400 MHz, DMSO-d_6): δ 8.81 (s, 2H), 6.74-6.70 (m, 2H), 6.62-6.59 (m, 2H).

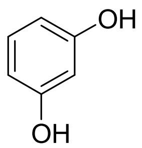

2t

2t,[5] white solid, IsoPOP-1: 19.8 mg, 90% yield; IsoPOP-2: 19.4 mg, 88% yield. ^{1}H NMR (400 MHz, DMSO-d_6): δ 9.15 (s, 2H), 6.93-6.89 (m, 1H), 6.20-6.17 (m, 3H).

5. General Procedure for Visible-Light-Induced Oxidation of Aldehydes

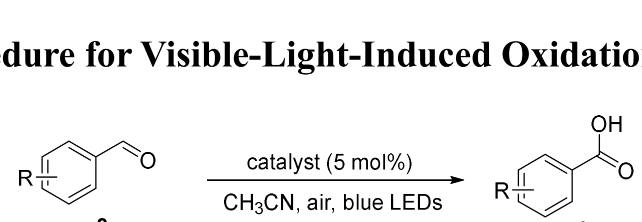

To a Schlenk tube were added the substrate **3** (0.2 mmol, 1.0 equiv), IsoPOP-1 or IsoPOP-2 (5 mol%), and acetonitrile (2 mL). The reaction mixture was positioned approximately 2~3 cm from a 30 W blue LEDs lamp under air. The mixture was stirred at room temperature for the indicated time (monitored by TLC). Afterwards, the catalyst was separated by microcentrifuge and washed with dichloromethane. Then the filtrate was concentrated by rotary evaporation and the residue was purified by silica gel flash column chromatography using ethyl acetate/petroleum ether as the eluent to afford the desired products **4**. The analytical data of the products are summarized below.

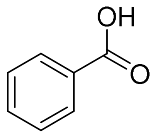

4a

4a,[5] white solid, IsoPOP-1: 24.2 mg, 99% yield; IsoPOP-2: 24.2 mg, 99% yield. ^{1}H NMR (400 MHz, $CDCl_3$): δ 8.13 (d, J = 7.2 Hz, 2H), 7.63 (t, J = 7.6 Hz, 1H), 7.49 (t, J = 7.6 Hz, 2H).

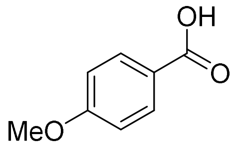

4b

4b,[5] white solid, IsoPOP-1: 29.8 mg, 98% yield; IsoPOP-2: 28.3 mg, 93% yield. ^{1}H NMR (400 MHz, $CDCl_3$): δ 8.07 (d, J = 9.2 Hz, 2H), 6.95 (d, J = 8.8 Hz, 2H), 3.88 (s, 3H).

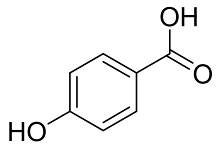

4c

4c,[5] white solid, IsoPOP-1: 25.1 mg, 91% yield; IsoPOP-2: 23.5 mg, 85% yield. ^{1}H NMR (400 MHz, DMSO-d_6): δ 12.42 (br, 1H), 10.22 (br, 1H), 7.79 (d, J = 8.8 Hz, 2H), 6.82 (d, J = 8.4 Hz, 2H).

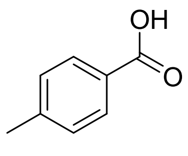

4d

4d,[5] white solid, IsoPOP-1: 27.0 mg, 99% yield; IsoPOP-2: 26.9 mg, 99% yield. ^{1}H NMR (400 MHz, $CDCl_3$): δ 8.00 (d, J = 8.4 Hz, 2H), 7.28 (d, J = 8.0 Hz, 2H), 2.44 (s, 3H).

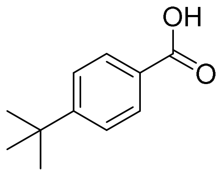

4e

4e,[6] white solid, IsoPOP-1: 35.3 mg, 99% yield; IsoPOP-2: 34.6 mg, 97% yield. ^{1}H NMR (400 MHz, DMSO-d_6): δ 12.79 (br, 1H), 7.88 (d, J = 8.8 Hz, 2H), 7.52 (d, J = 8.9 Hz, 2H), 1.30 (s, 9H).

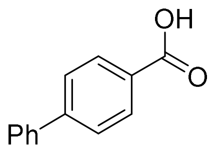

4f

4f,[6] white solid, IsoPOP-1: 39.2 mg, 99% yield; IsoPOP-2: 37.7 mg, 95% yield. ^{1}H NMR (400 MHz, DMSO-d_6) δ 12.99 (br, 1H), 8.02 (d, J = 8.4 Hz, 2H), 7.80 (d, J = 8.4 Hz, 2H), 7.74 (d, J = 6.8 Hz, 2H), 7.53-7.49 (m, 2H), 7.45-7.41 (m, 1H).

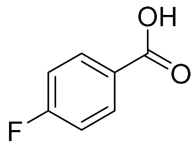

4g

4g,[5] white solid, IsoPOP-1: 25.8 mg, 92% yield; IsoPOP-2: 25.2 mg, 90% yield. ^{1}H NMR (400 MHz, DMSO-d_6) δ 13.05 (br, 1H), 8.03-7.98 (m, 2H), 7.33 (t, J = 8.8 Hz, 2H).

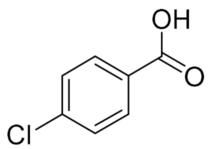

4h

4h,[5] white solid, IsoPOP-1: 28.2 mg, 90% yield; IsoPOP-2: 27.9 mg, 89% yield. ^{1}H NMR (400 MHz, DMSO-d_6) δ 12.19 (br, 1H), 7.94 (d, J = 8.4 Hz, 2H), 7.57 (d, J = 8.4 Hz, 2H).

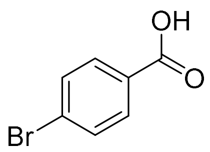

4i

4i,[5] white solid, IsoPOP-1: 36.2 mg, 90% yield; IsoPOP-2: 35.8 mg, 89% yield. ^1H NMR (400 MHz, $CDCl_3$) δ 7.95 (d, *J* = 8.4 Hz, 2H), 7.62 (d, *J* = 8.8 Hz, 2H).

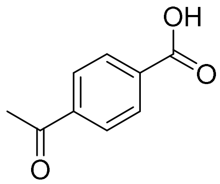

4j

4j,[6] white solid, IsoPOP-1: 29.5 mg, 90% yield; IsoPOP-2: 28.6 mg, 87% yield. ^1H NMR (400 MHz, DMSO-d_6) δ 13.32 (br, 1H), 8.06 (s, 4H), 2.63 (s, 3H).

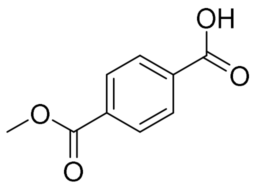

4k

4k,[6] white solid, IsoPOP-1: 30.6 mg, 85% yield; IsoPOP-2: 29.9 mg, 83% yield. ^1H NMR (400 MHz, $CDCl_3$) δ 8.15 (q, *J* = 8.4 Hz, 4H), 3.97 (s, 3H).

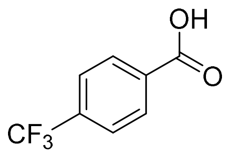

4l

4l,[6] white solid, IsoPOP-1: 33.8 mg, 89% yield; IsoPOP-2: 32.3 mg, 85% yield. ^1H NMR (400 MHz, $CDCl_3$) δ 8.24 (d, *J* = 8.0 Hz, 2H), 7.77 (d, *J* = 8.4 Hz, 2H).

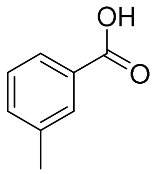

4m

4m, [6] white solid, IsoPOP-1: 26.7 mg, 98% yield; IsoPOP-2: 26.1 mg, 96% yield. ^{1}H NMR (400 MHz, $CDCl_3$) δ 7.93 (d, *J* = 8.4 Hz, 2H), 7.45-7.36 (m, 2H), 2.43 (s, 3H).

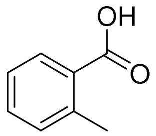

4n

4n,[6] white solid, IsoPOP-1: 27.0 mg, 99% yield; IsoPOP-2: 26.4 mg, 97% yield. ^{1}H NMR (400 MHz, $CDCl_3$) δ 8.08 (d, *J* = 6.4 Hz, 1H), 7.46 (t, *J* = 7.6 Hz, 1H), 7.29 (t, *J* = 6.8 Hz, 2H), 2.67 (s, 3H).

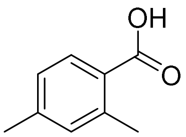

4o

4o,[6] white solid, IsoPOP-1: 28.5 mg, 95% yield; IsoPOP-2: 27.3 mg, 91% yield. ^{1}H NMR (400 MHz, $CDCl_3$) δ 7.97 (d, *J* = 8.4 Hz, 1H), 7.10-7.08 (m, 2H), 2.63 (s, 3H), 2.37 (s, 3H).

6. Recyclability Tests of IsoPOP-1 and IsoPOP-2

Table S4 Recyclability tests of IsoPOP-1 and IsoPOP-2 in oxidative hydroxylation of phenylboronic acid.

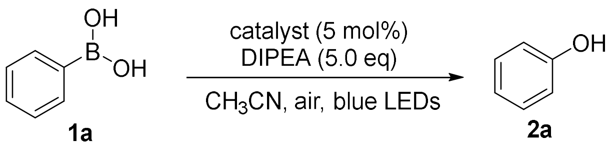

cycle	IsoPOP-1		IsoPOP-2	
	t (h)	yield (%)	*t* (h)	yield (%)
1	1	99	1.5	99
2	1	99	1.5	99
3	1	98	1.5	99
4	1	99	1.5	99
5	1	98	1.5	99
6	1	99	1.5	99
7	1	99	1.5	99
8	1.5	99	1.5	98
9	1.5	98	2	98
10	1.5	97	2	97
11	1.5	97	2	96
12	1.5	98	2	96
13	2	96	2.5	94
14	2	96	2.5	95
15	2	96	2.5	94

Table S5 Recyclability tests of IsoPOP-1 and IsoPOP-2 in oxidation of benzaldehyde.

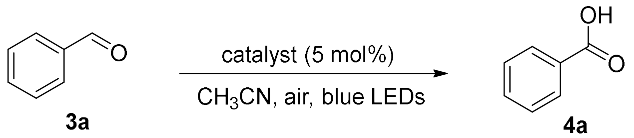

cycle	IsoPOP-1		IsoPOP-2	
	t (h)	yield (%)	*t* (h)	yield (%)
1	12	99	15	99
2	12	99	15	99
3	12	99	15	99
4	12	98	15	99
5	12	98	15	98
6	12	99	15	99
7	12	99	15	99
8	12	99	15	98
9	13	99	15	99
10	13	98	16	97
11	15	97	16	95
12	15	97	17	96
13	15	96	17	94
14	15	97	19	93
15	17	95	19	93

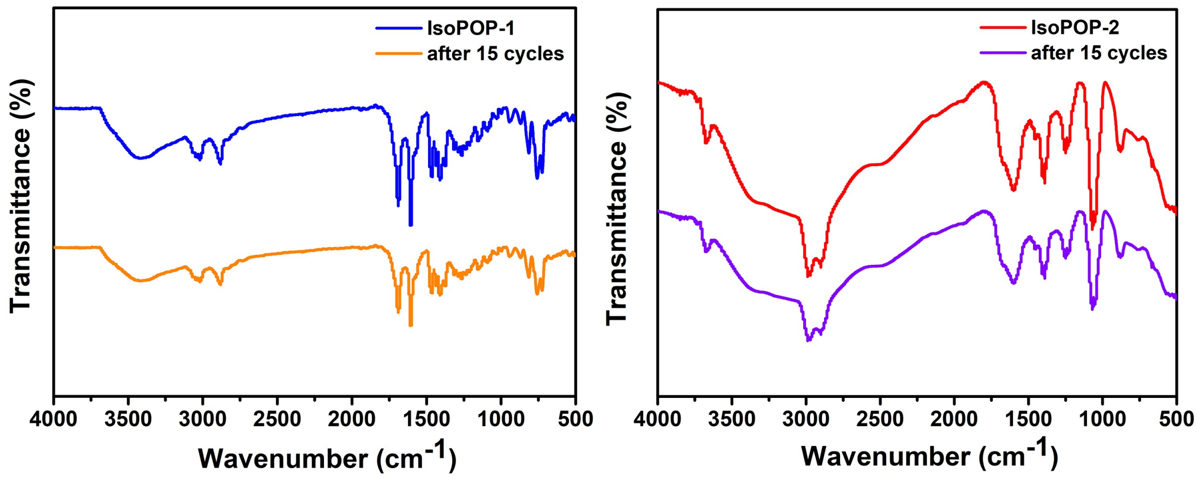

Fig. S13 FTIR spectra of IsoPOP-1 and IsoPOP-2 after 15 cycles of the reaction.

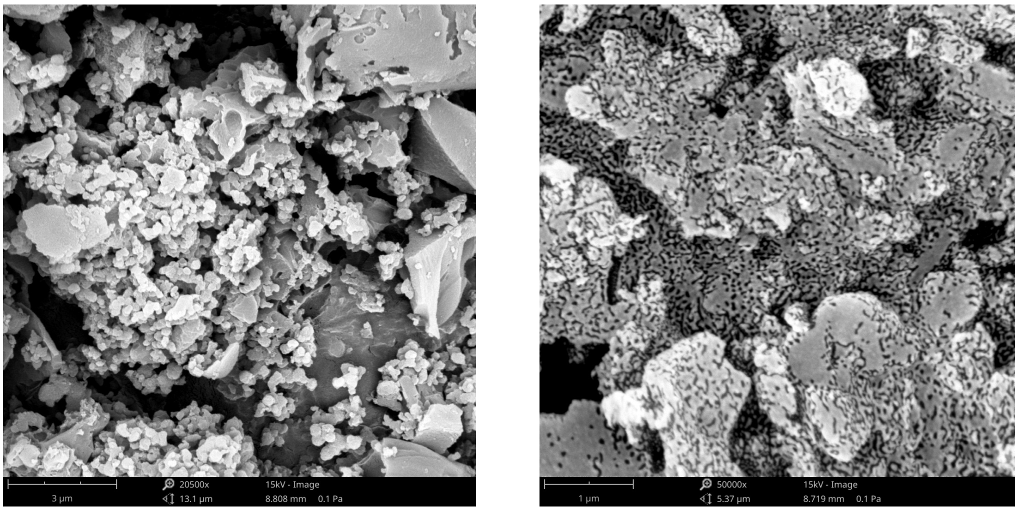

Fig. S14 SEM images of IsoPOP-1 and IsoPOP-2 after 15 cycles of the reaction.

7. Mechanistic Studies

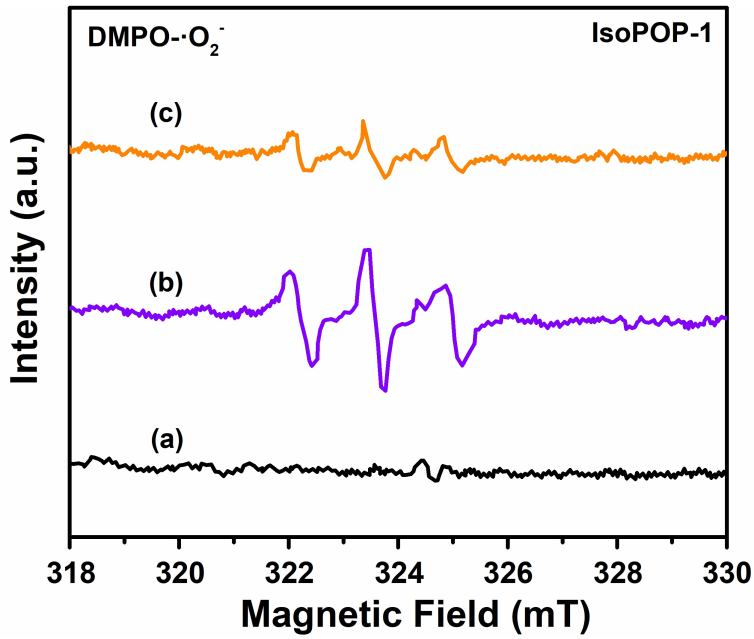

Fig. S15 ESR spectra of (a) DMPO (0.02 M) and DIPEA (0.5 M) in air-saturated CH_3CN; (b) DMPO (0.02 M), DIPEA (0.5 M) and IsoPOP-1 (2.2 mg/mL, based on monomer) in air-saturated CH_3CN; and (c) DMPO (0.02 M), DIPEA (0.5 M), IsoPOP-1 (2.2 mg/mL, based on monomer) and phenylboronic acid (0.1 M) in air-saturated CH_3CN. All the irradiations were performed with blue LEDs at room temperature for 30 min. The mixture was separated by filtration and the supernatant was subjected to the ESR measurement. [16]

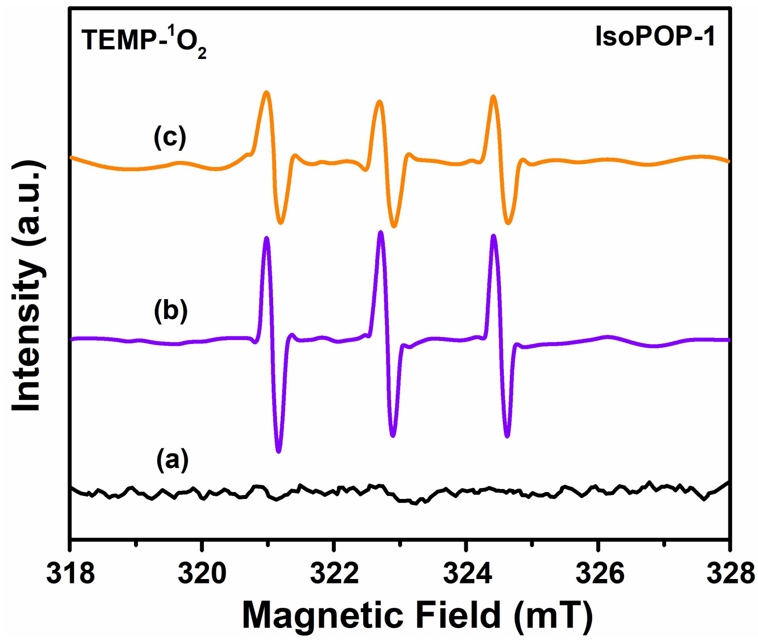

Fig. S16 ESR spectra of (a) TEMP (0.02 M) in air-saturated CH_3CN; (b) TEMP (0.02 M) and IsoPOP-1 (2.2 mg/mL, based on monomer) in air-saturated CH_3CN; and (c) TEMP (0.02 M), IsoPOP-1 (2.2 mg/mL, based on monomer) and benzaldehyde (0.1 M) in air-saturated CH_3CN. All the irradiations were performed with blue LEDs at room temperature for 1 h. The mixture was separated by filtration and the supernatant was subjected to the ESR measurement.[16]

8. Comparision with Known Photocatalysts

Table S6 Comparision with known photocatalysts for oxidative hydroxylation of phenylboronic acid.

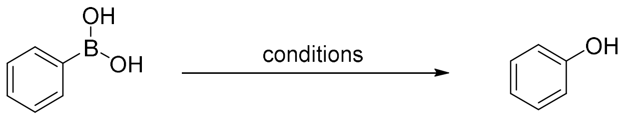

entry	catalyst	specific surface area ($m^2 \cdot g^{-1}$)	*t* (h)	solvent	light	yield (%)	TON	TOF (h^{-1})	ref
1	IsoPOP-1	727	1	CH_3CN	30 W blue LEDs	99	19.8	19.8	this work
2	IsoPOP-2	543	1.5	CH_3CN	30 W blue LEDs	99	19.8	13.2	
3	Cz-POF-1	2065	24	DMF	14 W compact fluorescent lamp	94	47.0	1.96	[7]
4	PCP-MF	130	10	CH_3CN	white LED lamp	94	52.2	5.52	[8]
5	CPOP-29	76	48	DMF	23 W white LED lamp	98	49.0	1.02	[9]
6	LZU-190	1035	48	CH_3CN/H_2O	20 W white LEDs	99	13.3	0.28	
7	LZU-191	1035	48	CH_3CN/H_2O	20 W white LEDs	99	20	0.42	[10]
8	LZU-192	706	48	CH_3CN/H_2O	20 W white LEDs	99	20	0.42	
9	BBO−COF	1070	96	CH_3CN/H_2O	18 W white LED	99	19.8	0.21	[11]
10	Ir-POP-2	124	24	CH_3CN	blue LED lamp	99	99	4.13	[2]
11^{c}	Tx-COF-2	1137	72	CH_3CN/H_2O	20 W white LEDs	74	7.4	0.10	[12]
12^{c}	COF-JLU25	141.31	72	CH_3CN/D_2O	20 W white LEDs	99	63.5	0.88	[13]

Table S7 Comparision with known photocatalysts for oxidation of benzaldehyde.

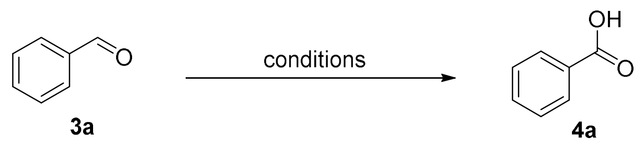

entry	catalyst	specific surface area ($m^2 \cdot g^{-1}$)	*t* (h)	solvent	light	yield (%)	TON	TOF (h^{-1})	ref
1	IsoPOP-1	727	12	CH_3CN	30 W blue LEDs	99	19.8	1.65	this work
2	IsoPOP-2	543	15	CH_3CN	30 W blue LEDs	99	19.8	1.32	
3	$Ir(dFppy)_3$	-	12	CH_3CN	blue LEDs	99	99.0	8.25	[6]
4	CPTF	117.2	4	CH_3CN	AM1.5G irradiation	87.1	449.0	112.25	[14]
5	CF_3SO_2Na	-	12	CH_3CN	blue LED (400-405 nm)	95	3.8	31.7	[15]
6	RGO-CoPcS	-	60	CH_3CN	288 power LED lamps	100	32.5	0.54	[5]

9. References

[1] T. Toyao, N. Ueno, K. Miyahara, Y. Matsui, T. Kim, Y. Horiuchi, H. Ikedaab and M. Matsuoka, *Chem. Commun.*, 2015, **51**, 16103-16106.

[2] Z.-Y. Xu, Y. Luo, D.-W. Zhang, H. Wang, X.-W. Sun and Z.-T. Li, *Green Chem.*, 2020, **22**, 136-143.

[3] L. Yang, Q. Zhuang, M. Wu, H. Long, C. Lin, M. Lin and F. Ke, *Org. Biomol. Chem.*, 2021, **19**, 6417-6421.

[4] S. Castellano and R. Kostelnik, *Tetrahedron Lett.*, 1867, **8**, 5211-5216.

[5] M. Hajimohammadi, N. Azizi, S. Tollabimazraeno, A. Tuna, J. Duchoslav and G. Knör, *Catal. Lett.*, 2021, **151**, 36-44.

[6] N. Iqbal, S. Choi, Y. You and E. J. Cho, *Tetrahedron Lett.*, 2013, **54**, 6222-6225.

[7] J. Luo, X. Zhang and J. Zhang, *ACS Catal.*, 2015, **5**, 2250-2254.

[8] Z. J. Wang, Run Li, K. Landfester and K. A. I. Zhang, *Polymer*, 2017, **126**, 291-295.

[9] H.-P. Liang, Q. Chen and B.-H. Han, *ACS Catal.*, 2018, **8**, 5313-5322.

[10] P.-F. Wei, M.-Z. Qi, Z.-P. Wang, S.-Y. Ding, W. Yu, Q. Liu, L.-K. Wang, H.-Z. Wang, W.-K. An and W. Wang, *J. Am. Chem. Soc.*, 2018, **140**, 4623-4631.

[11] X. Yan, H. Liu, Y. Li, W. Chen, T. Zhang, Z. Zhao, G. Xing and L. Chen, *Macromolecules*, 2019, **52**, 7977-7983.

[12] Y. Nailwal, A. D. D. Wonanke, M. A. Addicoat and S. K. Pal, *Macromolecules*, 2021, **54**, 6595-6604.

[13] G. Xiao, W. Li, T. Chen, W.-B. Hu, H. Yang, Y. A. Liu and K. Wen, *Eur. J. Org. Chem.*, 2021, **2021**, 3986-3991.

[14] W. Wu, S. Xu, G. Qi, H. Zhu, F. Hu, Z. Liu, D. Zhang and B. Liu, *Angew. Chem. Int. Ed.*, 2019, **58**, 3062-3066.

[15] X. Zhu, Y. Liu, C. Liu, H. Yang and H. Fu, *Green Chem.*, 2020, **22**, 4357-4363.

[16] (a) Y. Zhi, S. Ma, Hong Xia, Y. Zhang, Z. Shi, Y. M and X. Liu, *Appl. Catal. B: Environ.*, 2019, **244**, 36-44; (b) W. Zhang, S. Li, X. Tang, J. Tang, C, Pan, G. Yu, *Appl. Catal. B: Environ.*, 2020, **272**, 118982-118992; (c) C. Song, J. Nie, C. Ma, C. Lu, F. Wang, G. Yang, *Appl. Catal. B: Environ.*, 2021, **287**, 119984-119996.

10. Copies of NMR Spectra

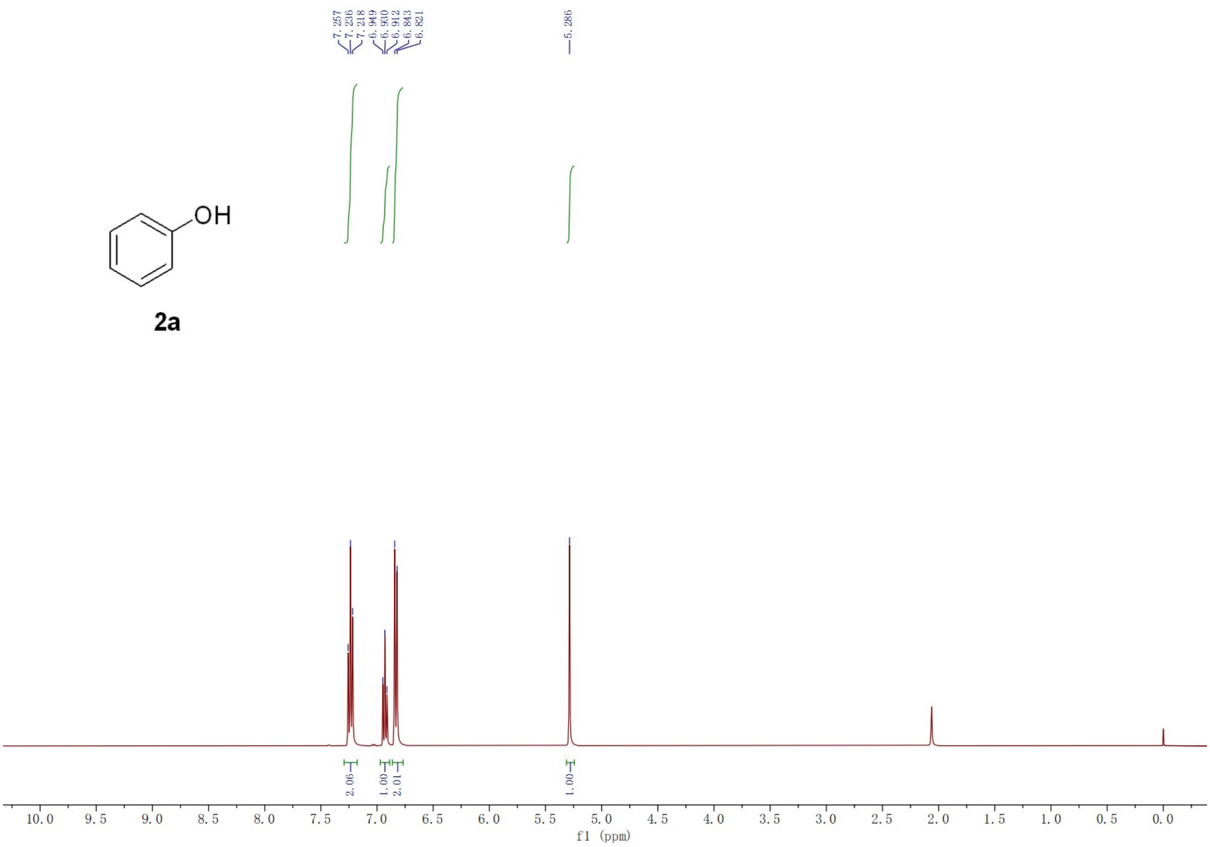

2a

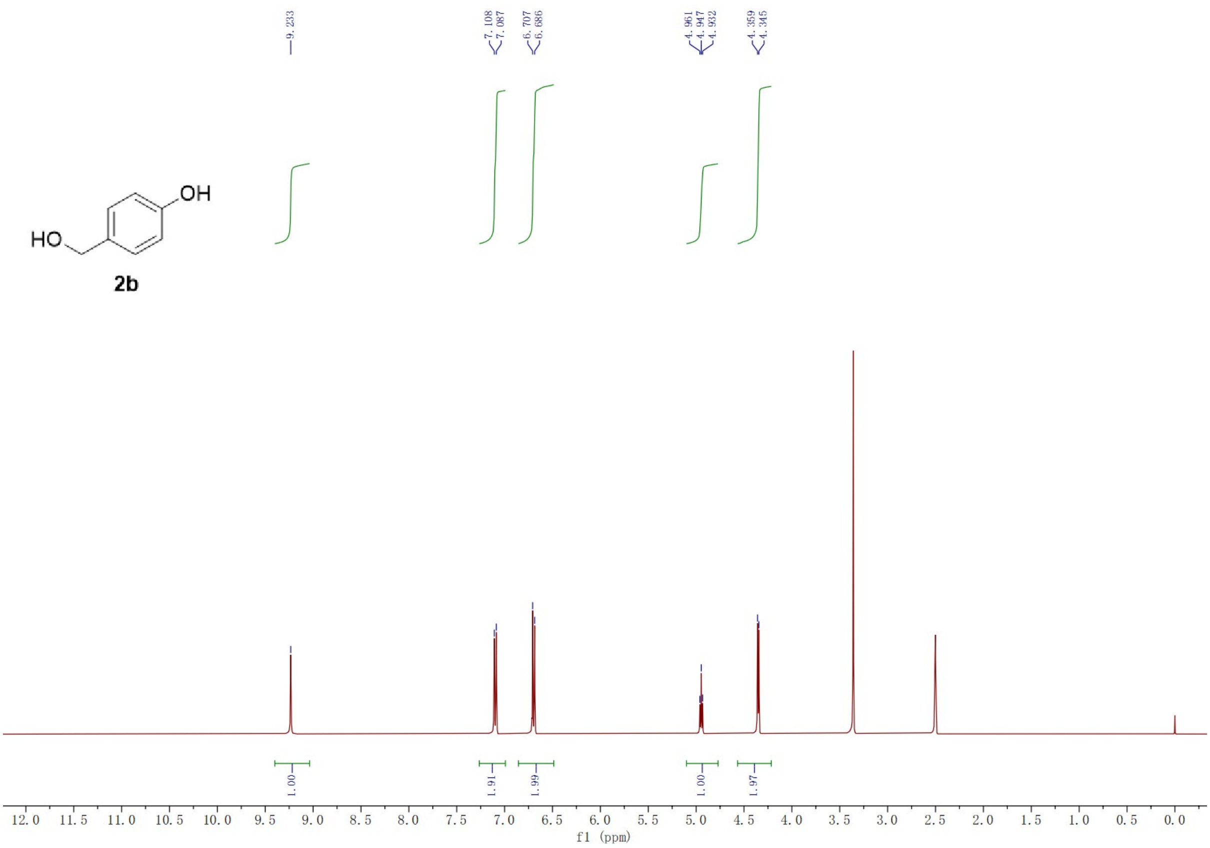

2b

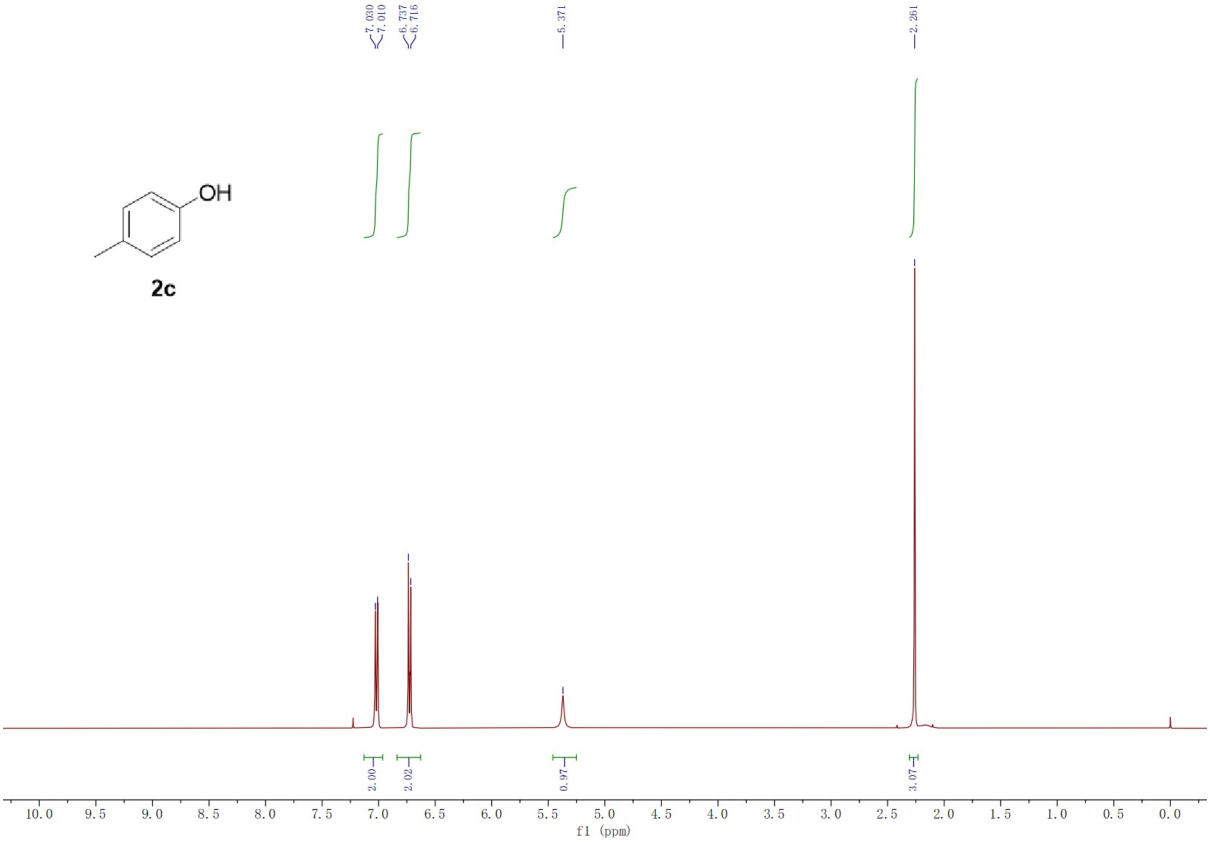
OH
2c
7.030
7.010
6.737
6.716
5.371
2.261
2.00
2.02
0.97
3.07
f1 (ppm)

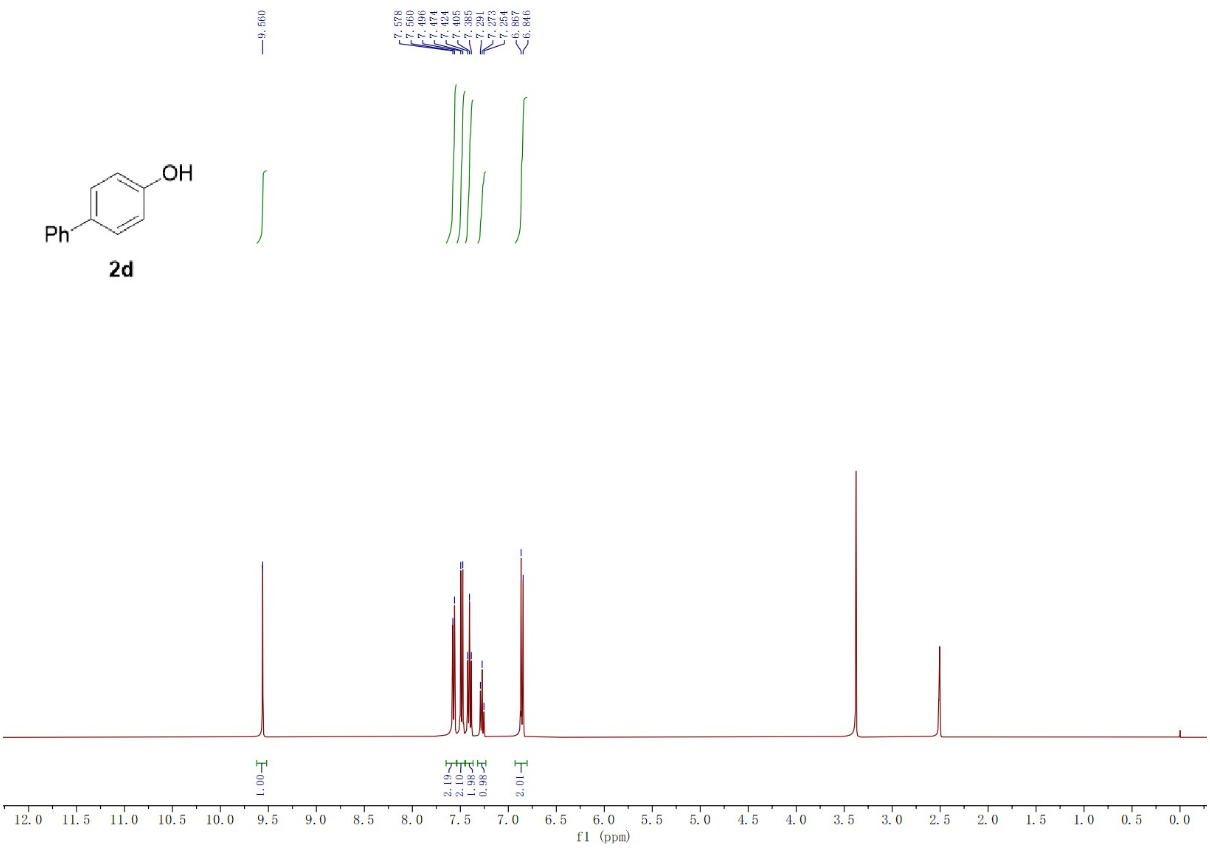
OH
Ph
2d
9.560
7.578
7.560
7.496
7.474
7.424
7.405
7.385
7.291
7.273
7.254
6.867
6.846
1.00
2.19
2.10
1.98
0.98
2.01
f1 (ppm)

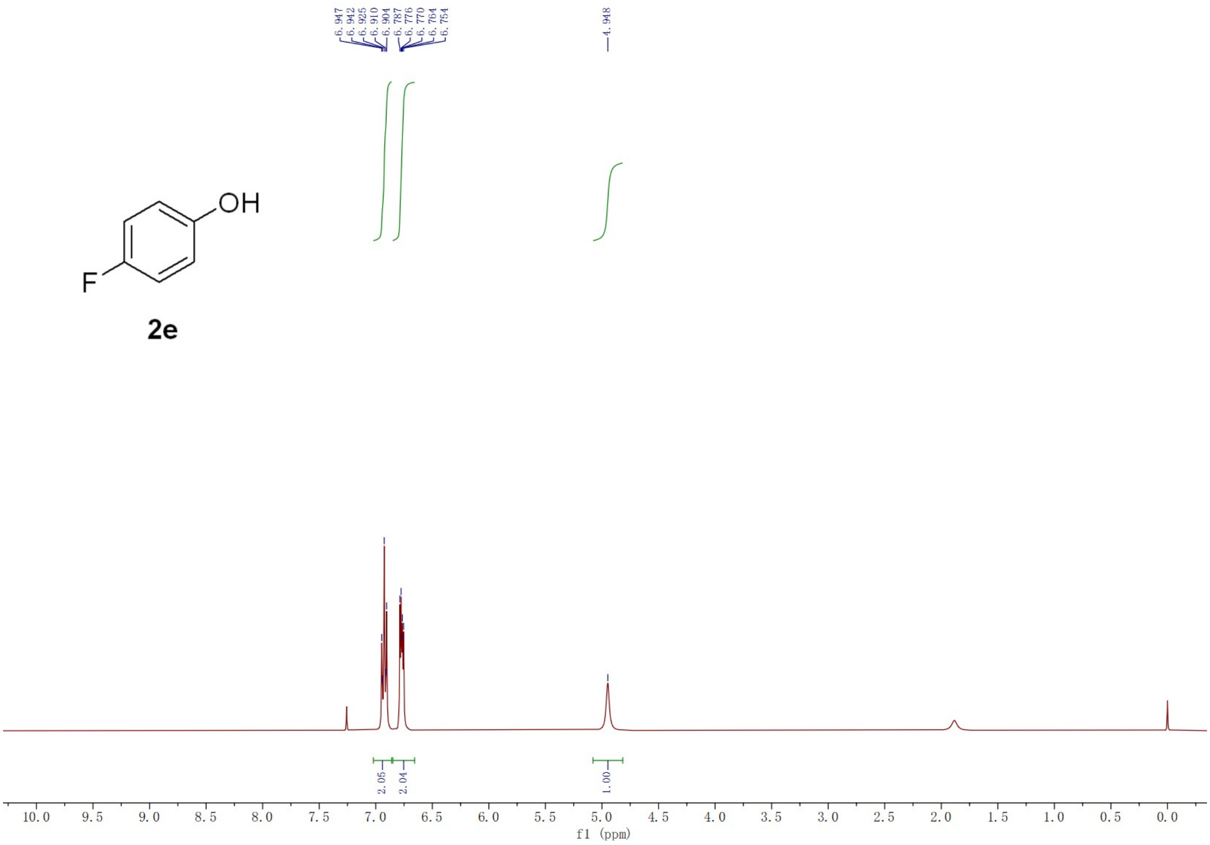
OH
F
6.947
6.942
6.925
6.910
6.904
6.787
6.776
6.770
6.764
6.754
4.948
2.05
2.04
1.00
f1 (ppm)

2e

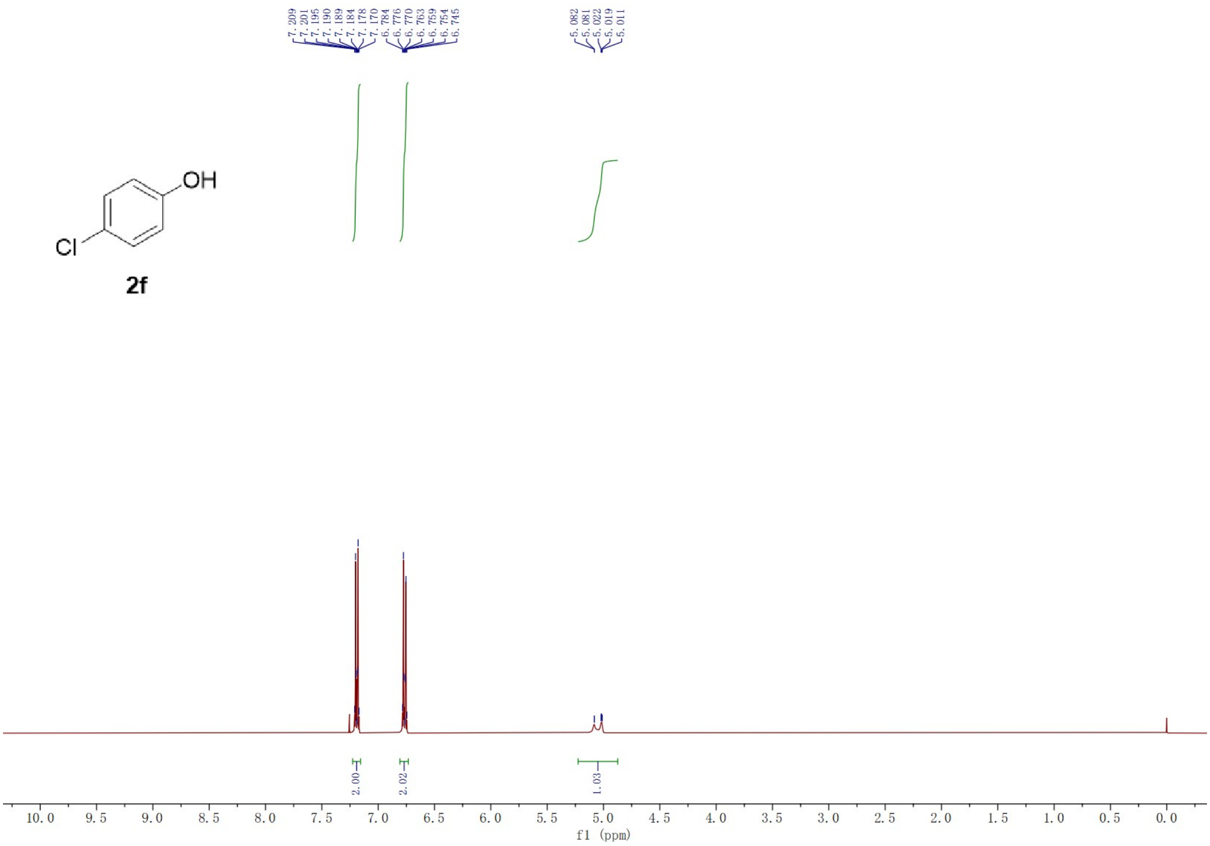
OH
Cl
7.209
7.201
7.195
7.190
7.189
7.184
7.178
7.170
6.784
6.776
6.770
6.763
6.759
6.754
6.745
5.082
5.081
5.022
5.019
5.011
2.00
2.02
1.03
f1 (ppm)

2f

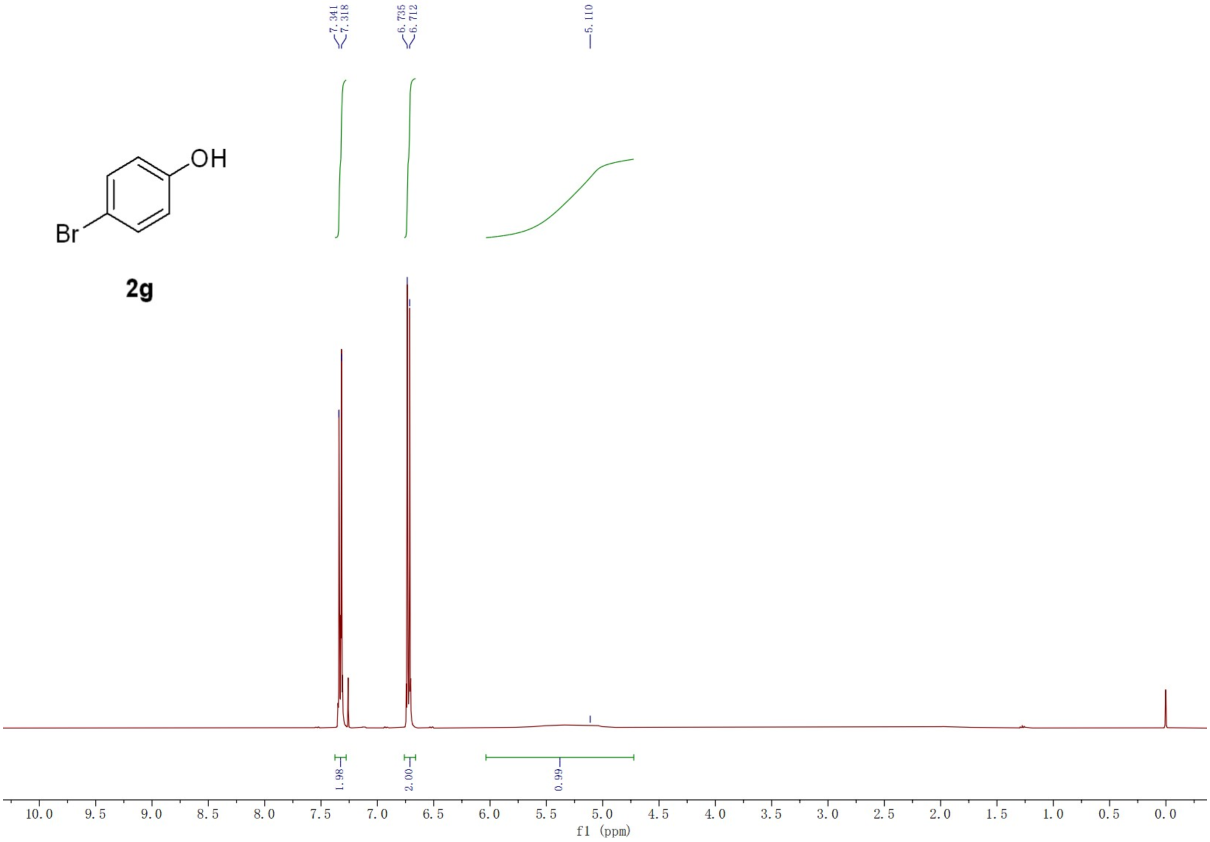

2g

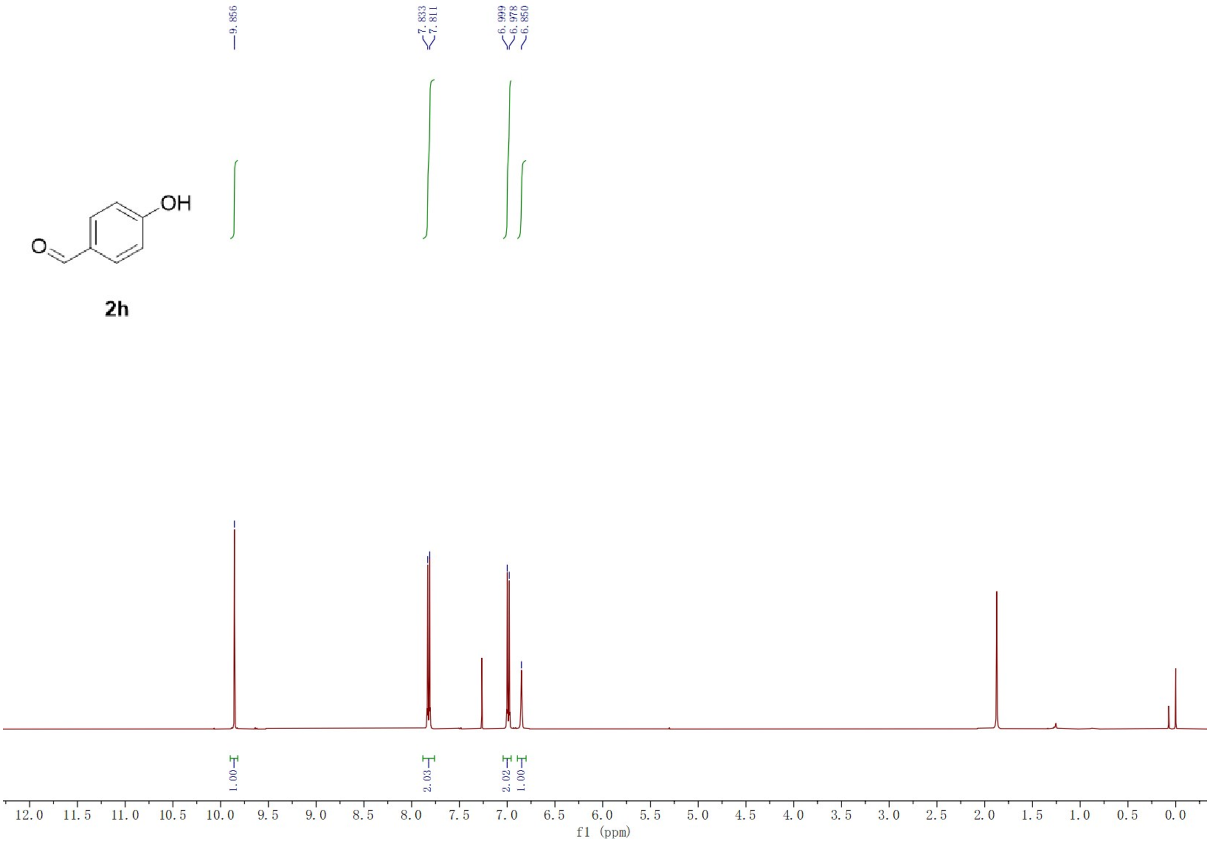

2h

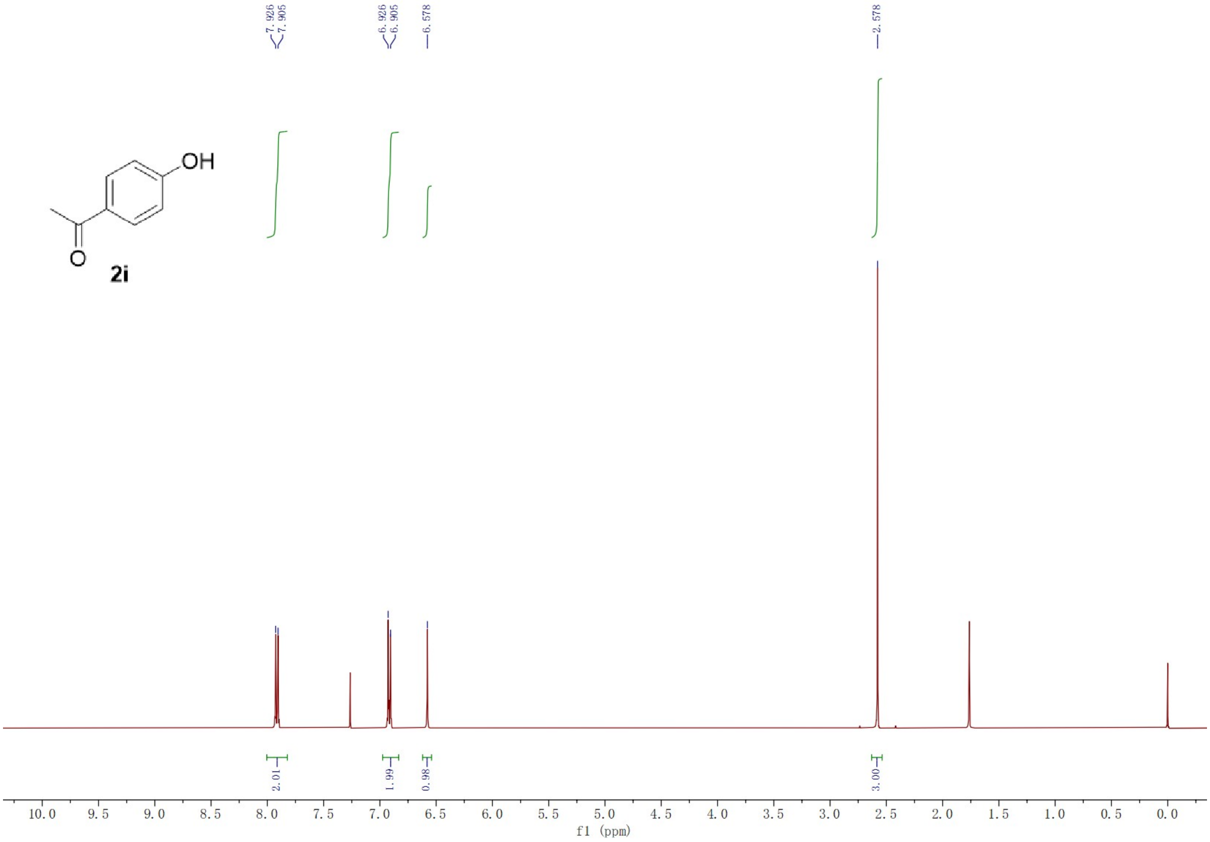
7.926
7.905
6.926
6.905
6.578
2.578
OH
O
2i
2.01
1.99
0.98
3.00
10.0 9.5 9.0 8.5 8.0 7.5 7.0 6.5 6.0 5.5 5.0 4.5 4.0 3.5 3.0 2.5 2.0 1.5 1.0 0.5 0.0
f1 (ppm)

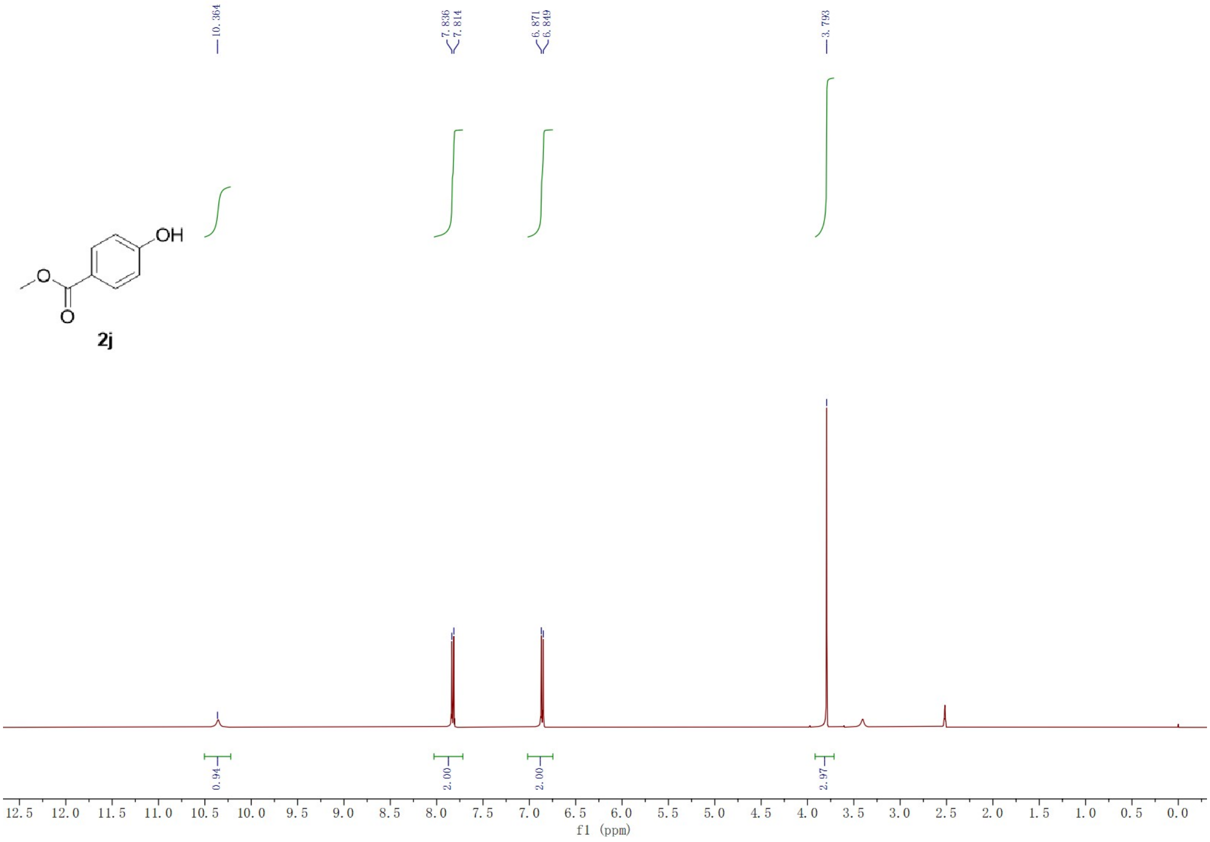
10.364
7.836
7.814
6.871
6.849
3.793
OH
O
O
2j
0.94
2.00
2.00
2.97
12.5 12.0 11.5 11.0 10.5 10.0 9.5 9.0 8.5 8.0 7.5 7.0 6.5 6.0 5.5 5.0 4.5 4.0 3.5 3.0 2.5 2.0 1.5 1.0 0.5 0.0
f1 (ppm)

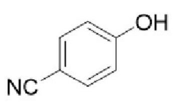
NC
OH

2k

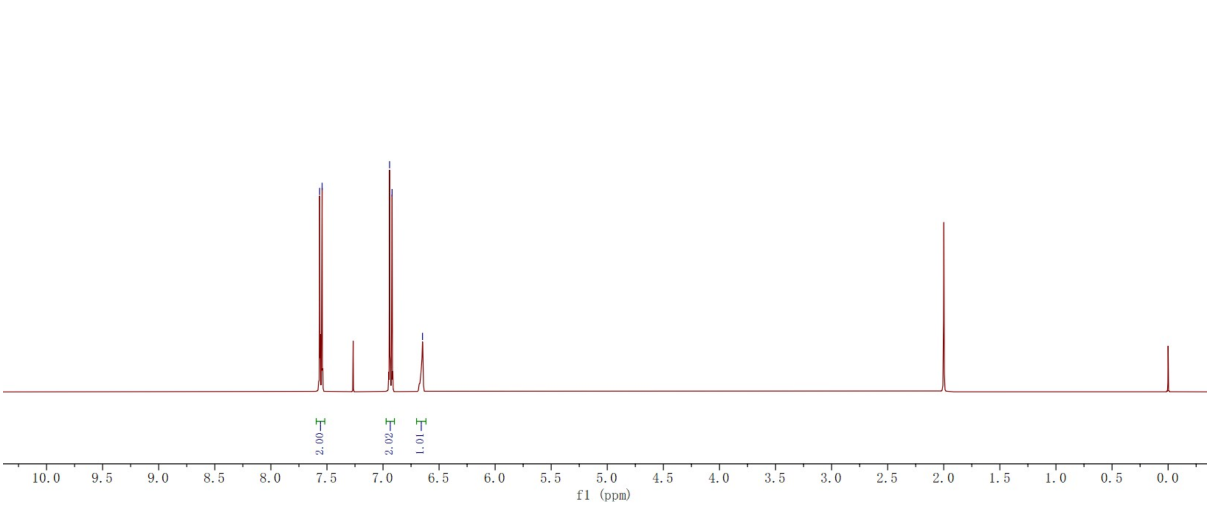
7.565
7.543
6.941
6.919
6.648
2.00
2.02
1.01
10.0 9.5 9.0 8.5 8.0 7.5 7.0 6.5 6.0 5.5 5.0 4.5 4.0 3.5 3.0 2.5 2.0 1.5 1.0 0.5 0.0
f1 (ppm)

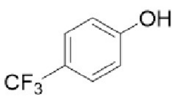
CF_3
OH

2l

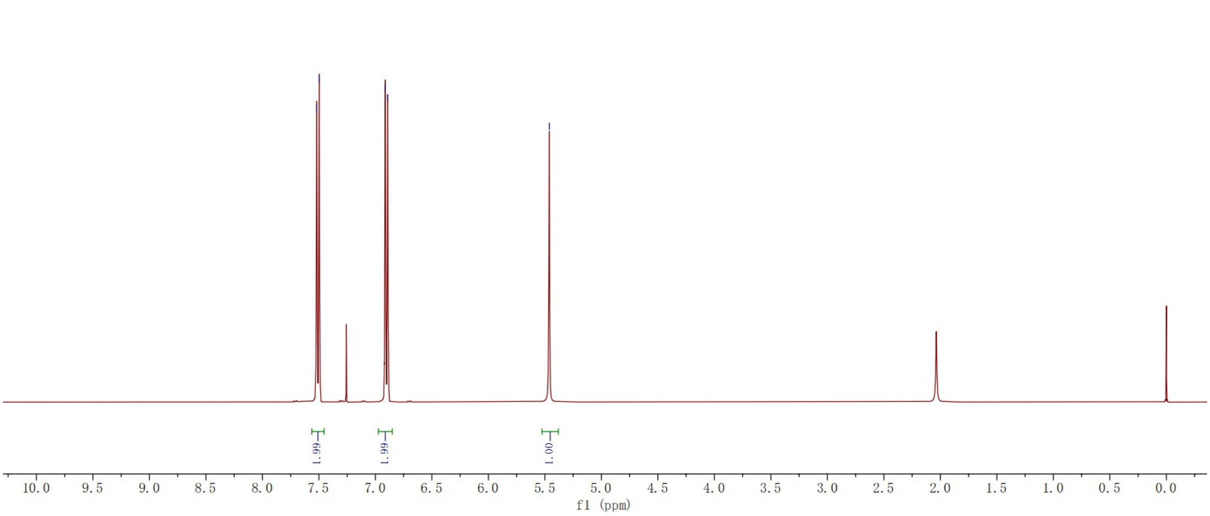
7.518
7.498
6.911
6.891
5.461
1.99
1.99
1.00
10.0 9.5 9.0 8.5 8.0 7.5 7.0 6.5 6.0 5.5 5.0 4.5 4.0 3.5 3.0 2.5 2.0 1.5 1.0 0.5 0.0
f1 (ppm)

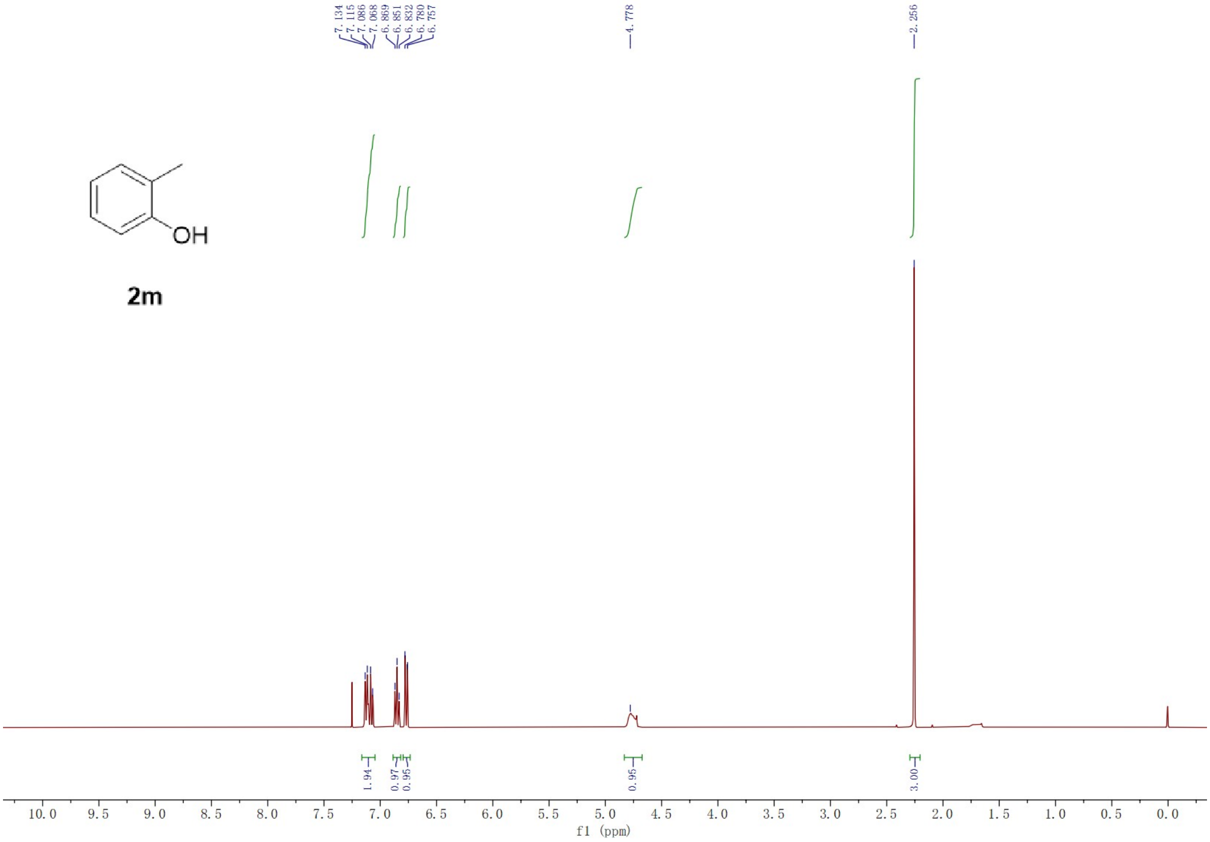
7.134
7.115
7.086
7.068
6.869
6.851
6.832
6.780
6.757
4.778
2.256
1.94
0.97
0.95
0.95
3.00
10.0 9.5 9.0 8.5 8.0 7.5 7.0 6.5 6.0 5.5 5.0 4.5 4.0 3.5 3.0 2.5 2.0 1.5 1.0 0.5 0.0
f1 (ppm)

2m

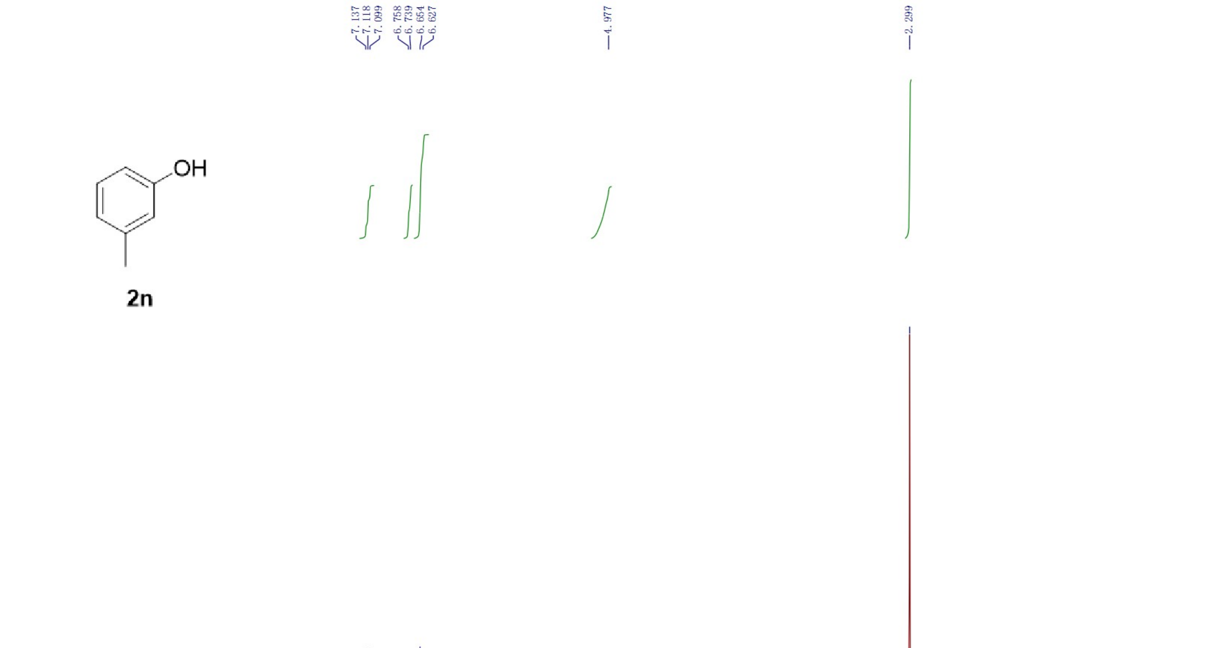
7.137
7.118
7.099
6.758
6.739
6.654
6.627
4.977
2.299
1.00
1.01
1.96
0.98
3.00
10.0 9.5 9.0 8.5 8.0 7.5 7.0 6.5 6.0 5.5 5.0 4.5 4.0 3.5 3.0 2.5 2.0 1.5 1.0 0.5 0.0
f1 (ppm)

2n

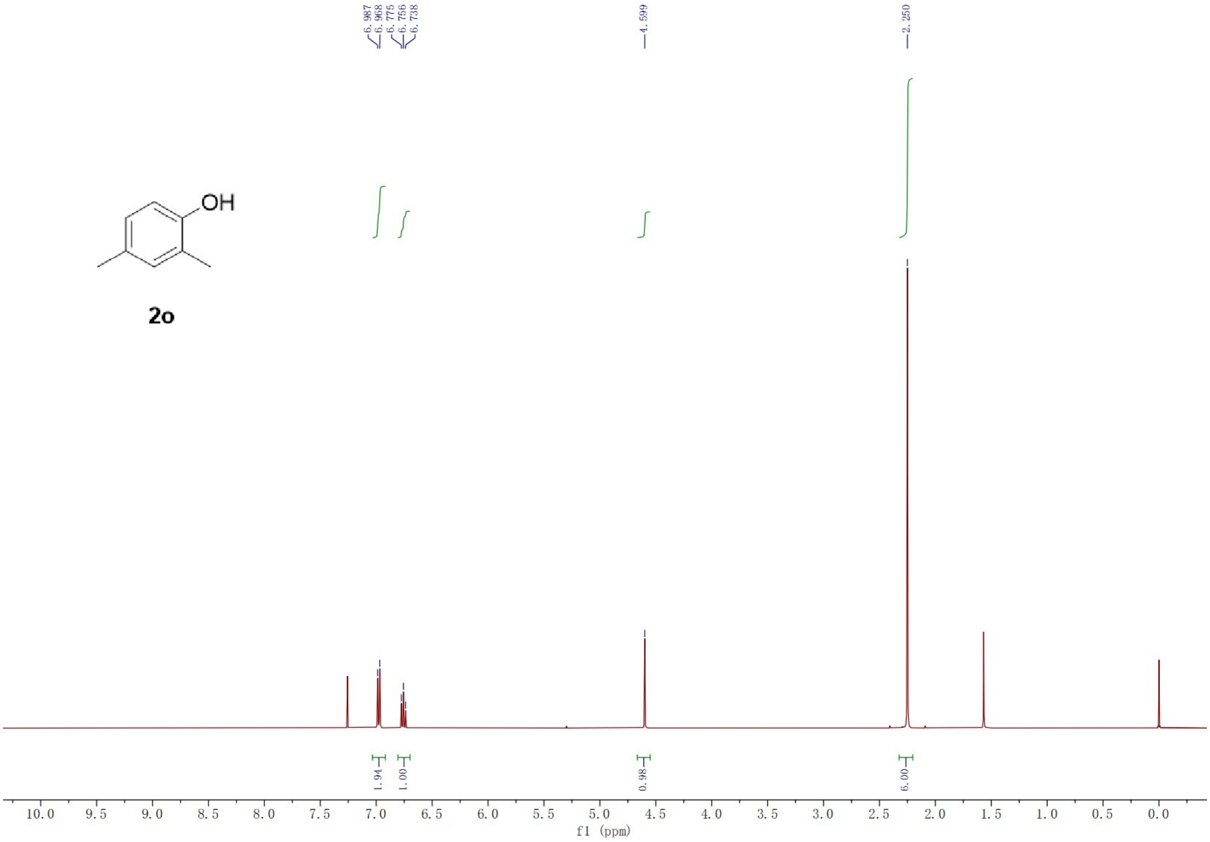
6.987
6.968
6.775
6.756
6.738
4.599
2.250
1.94
1.00
0.98
6.00
f1 (ppm)

2o

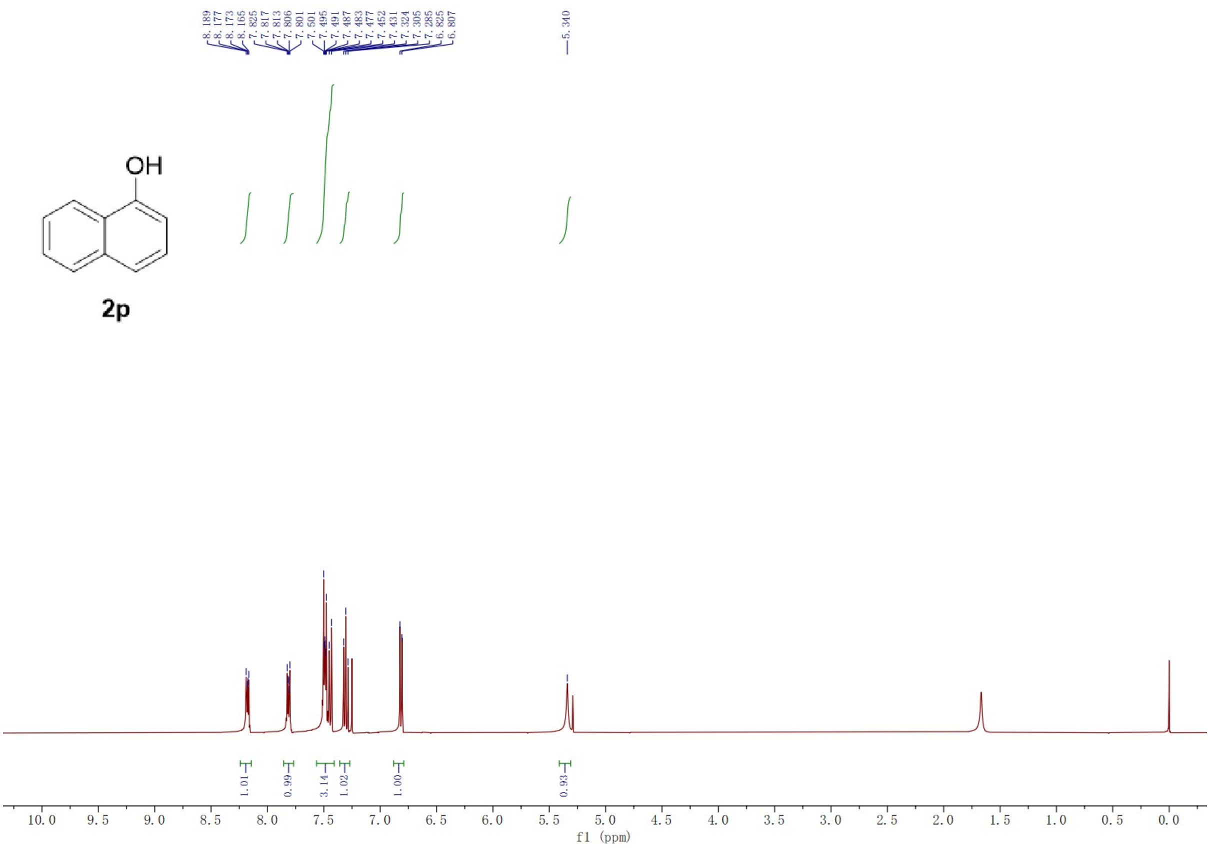
8.189
8.177
8.173
8.165
7.825
7.817
7.813
7.806
7.801
7.501
7.495
7.491
7.487
7.483
7.477
7.452
7.431
7.324
7.305
7.285
6.825
6.807
5.340
1.01
0.99
3.14
1.02
1.00
0.93
f1 (ppm)

2p

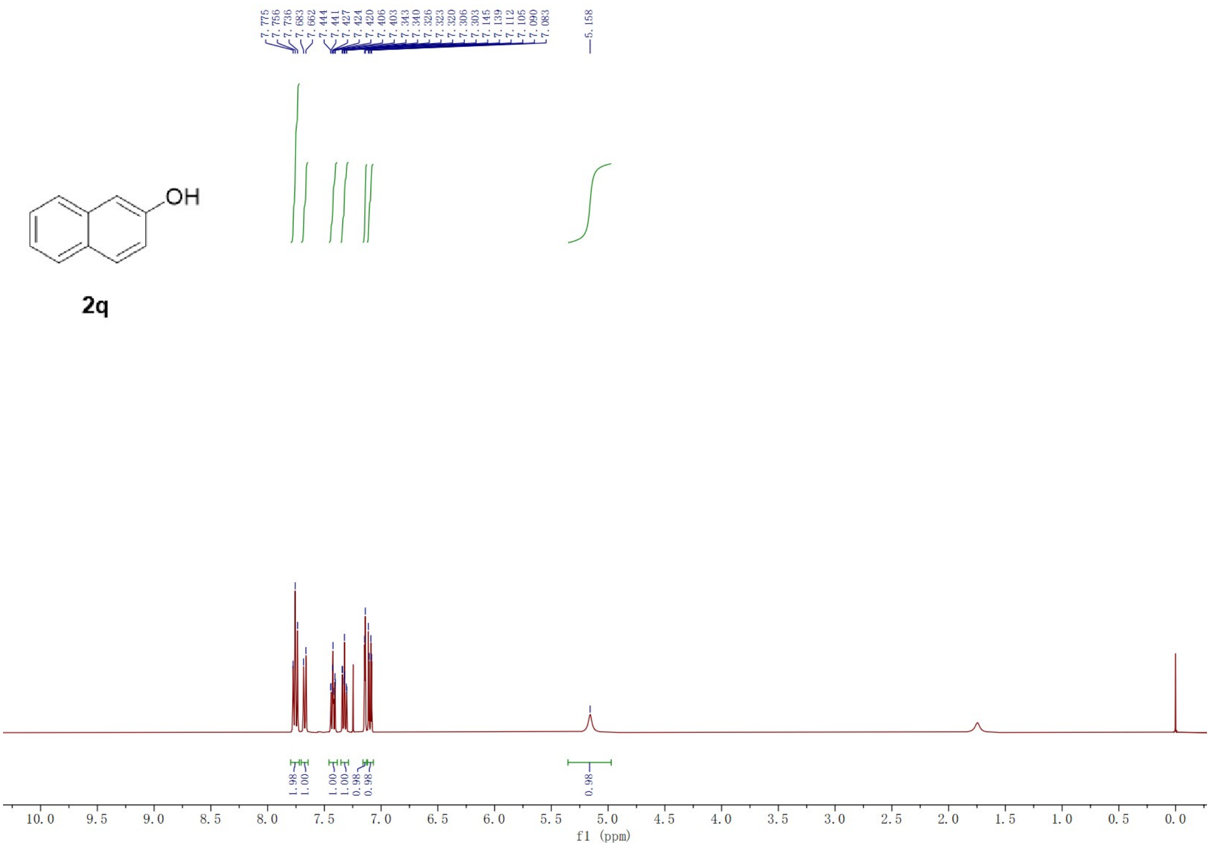
2q

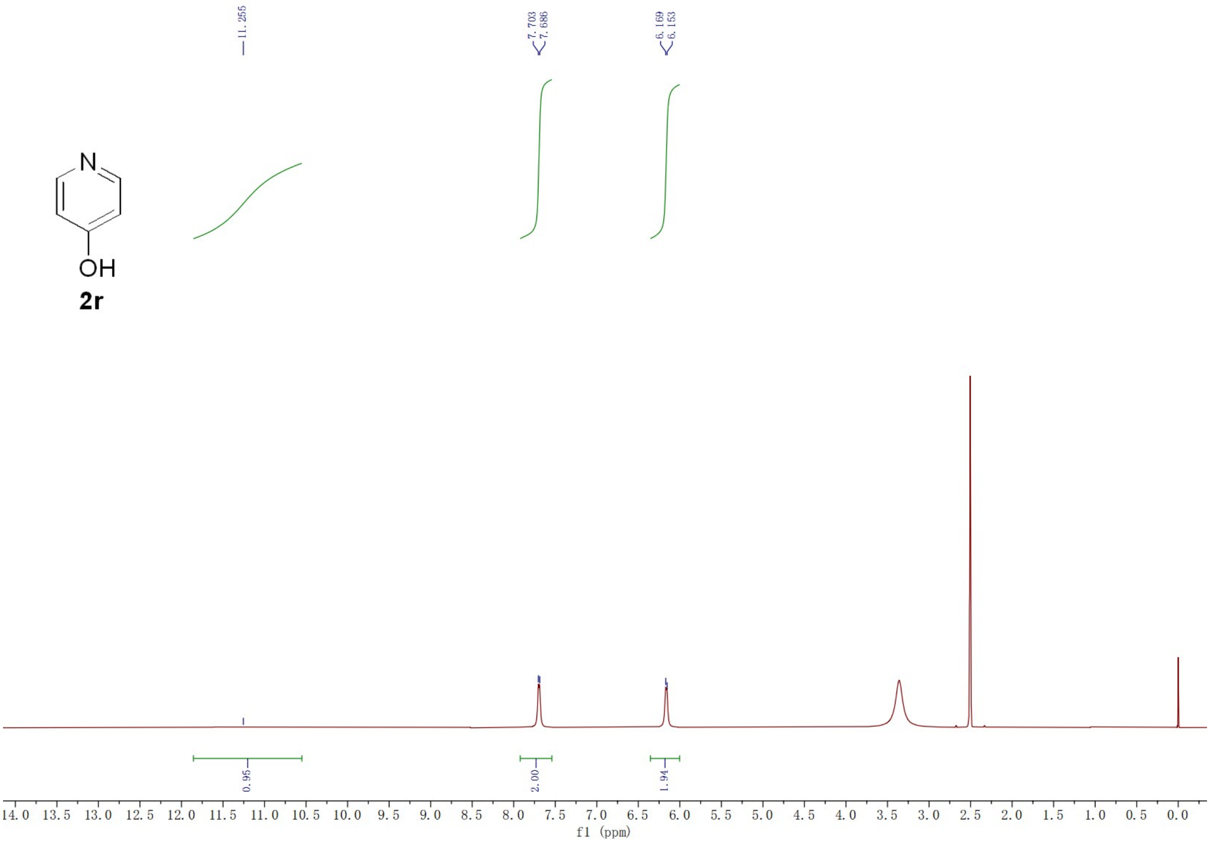
2r

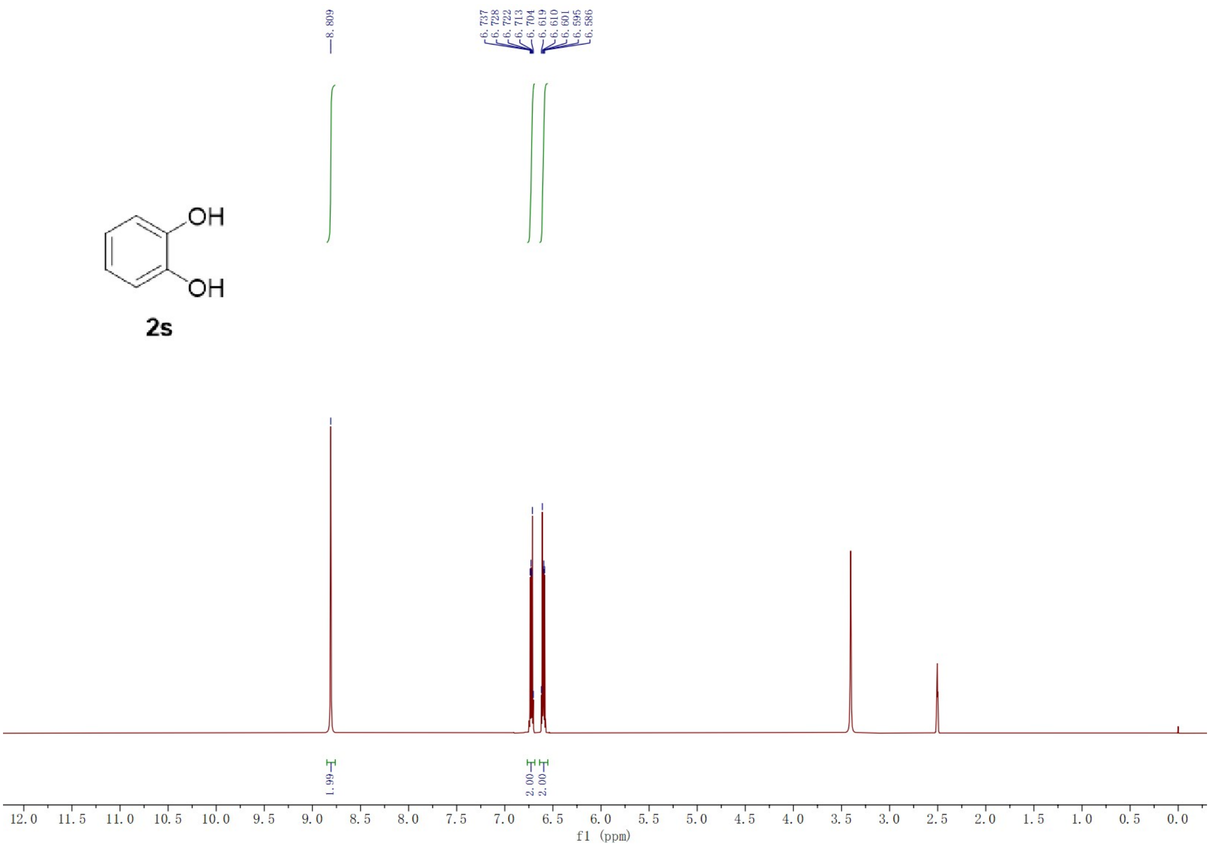
OH
OH
2s

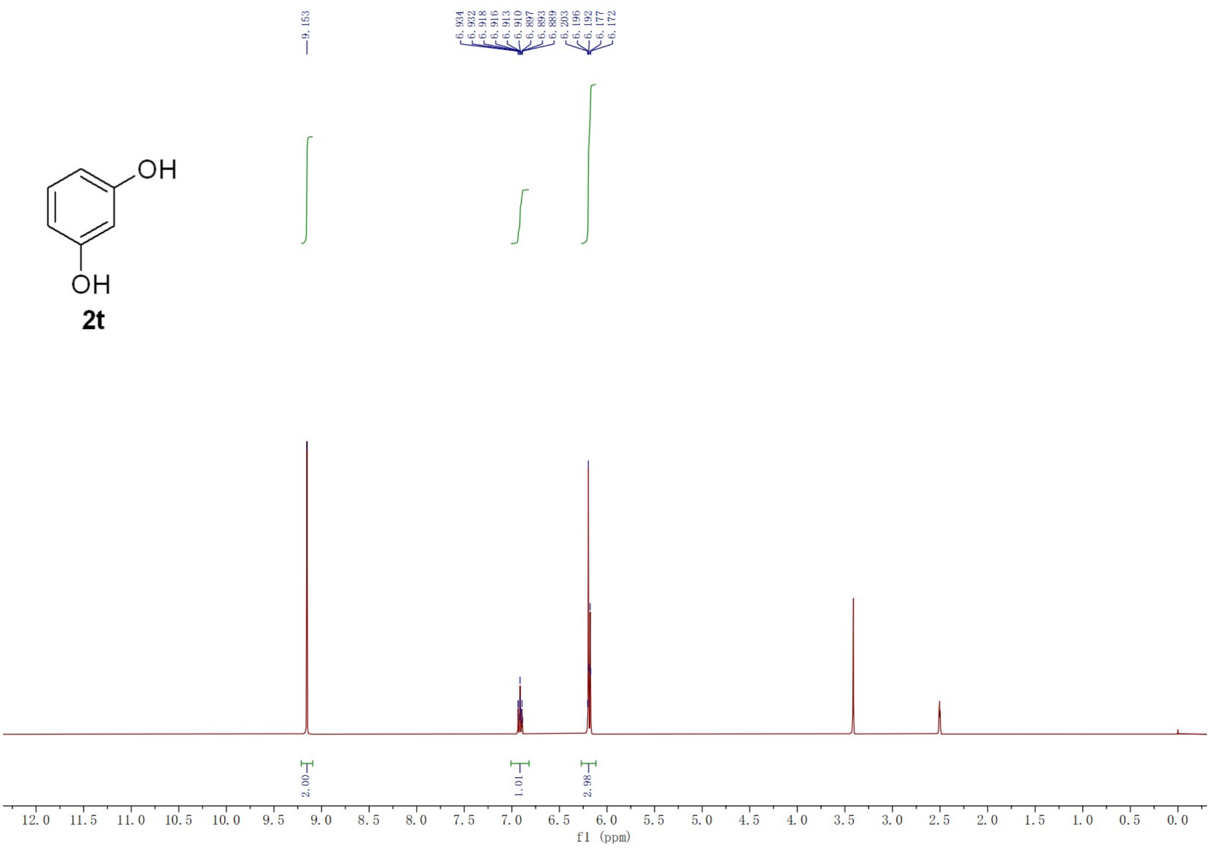
OH
OH
2t

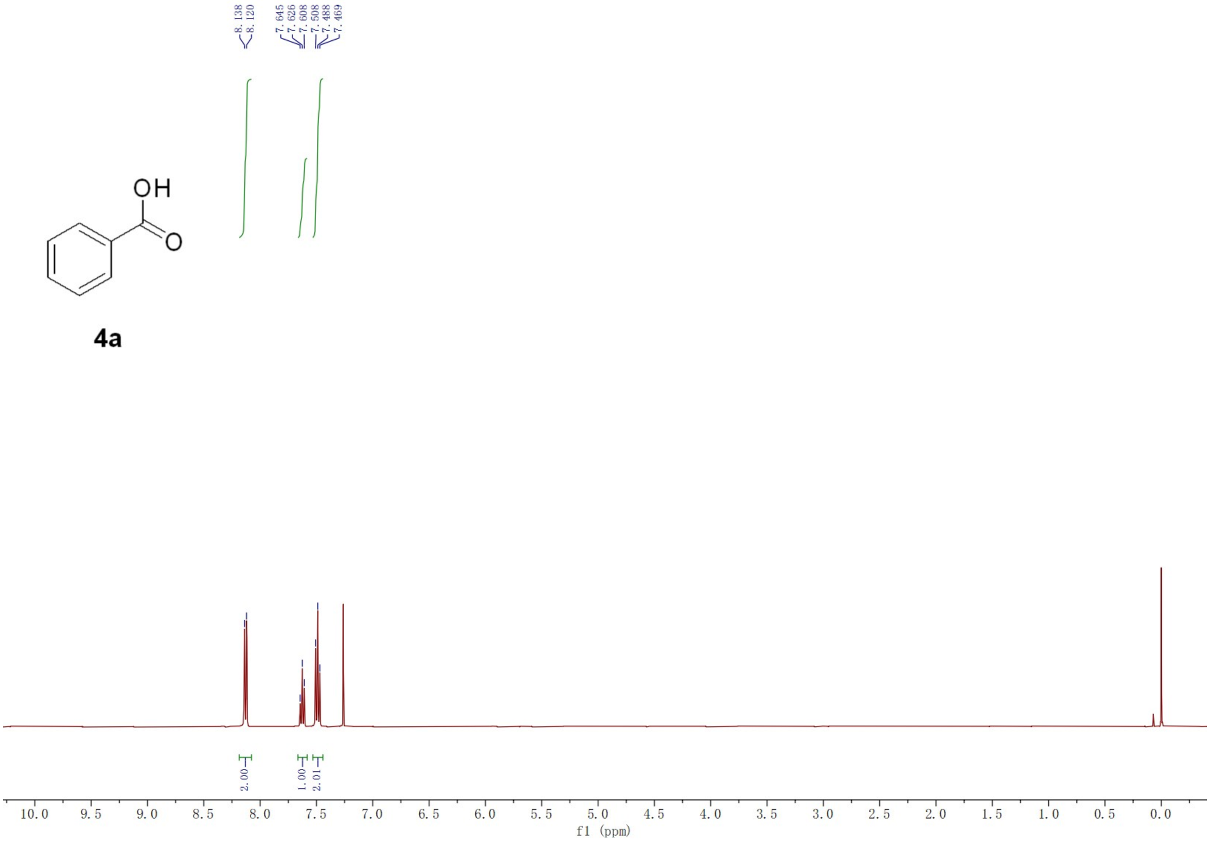

OH
O
8.138
8.120
7.645
7.626
7.608
7.508
7.488
7.469
2.00
1.00
2.01
10.0 9.5 9.0 8.5 8.0 7.5 7.0 6.5 6.0 5.5 5.0 4.5 4.0 3.5 3.0 2.5 2.0 1.5 1.0 0.5 0.0
f1 (ppm)

4a

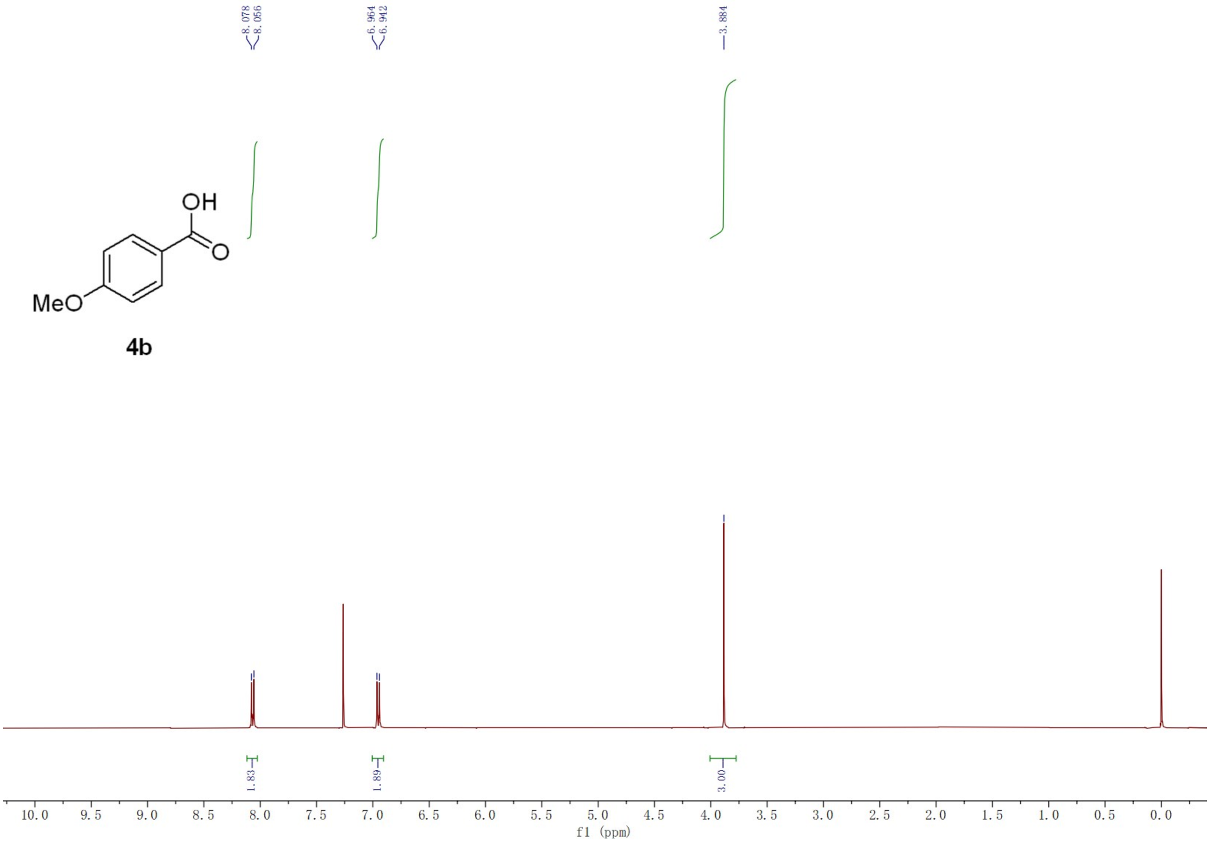

OH
O
MeO
8.078
8.056
6.964
6.942
3.884
1.83
1.89
3.00
10.0 9.5 9.0 8.5 8.0 7.5 7.0 6.5 6.0 5.5 5.0 4.5 4.0 3.5 3.0 2.5 2.0 1.5 1.0 0.5 0.0
f1 (ppm)

4b

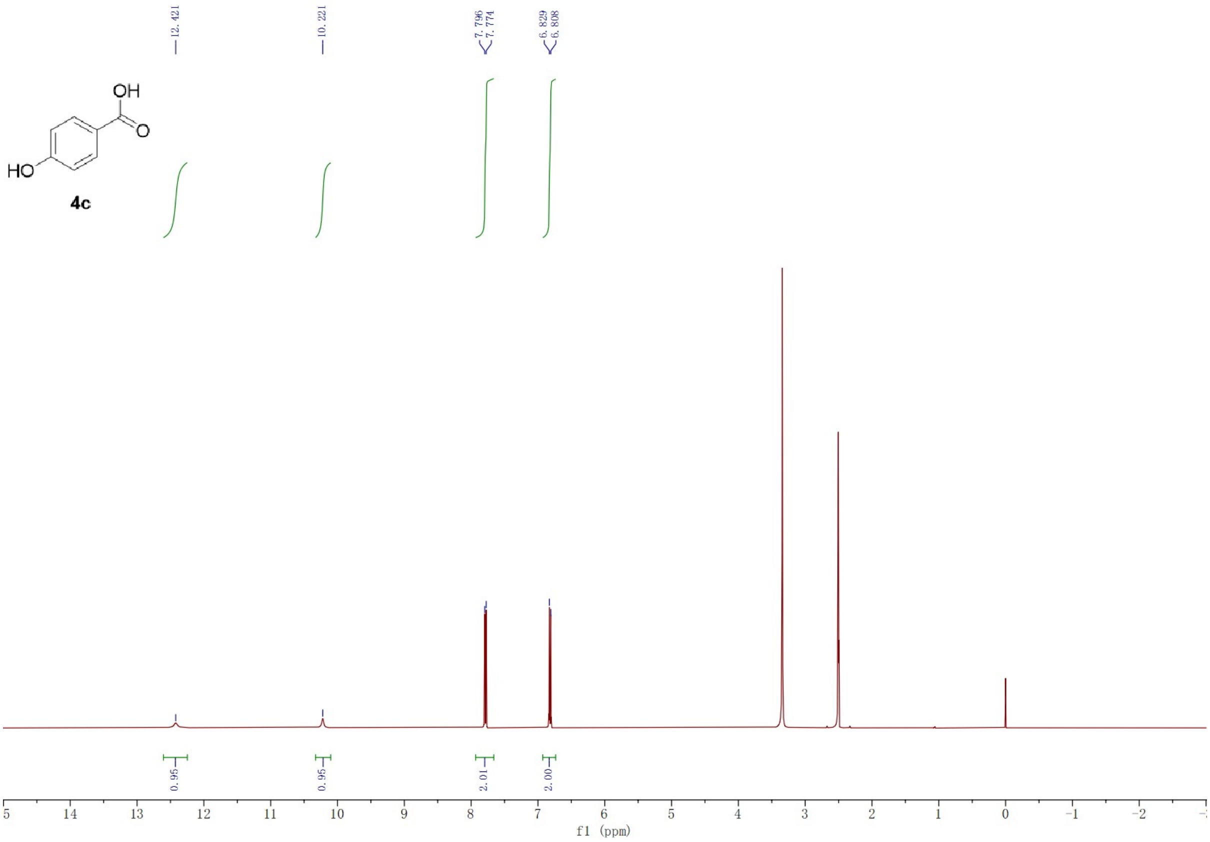

12.421
10.221
7.796
7.774
6.829
6.808
OH
O
HO
4c
0.95
0.95
2.01
2.00
15 14 13 12 11 10 9 8 7 6 5 4 3 2 1 0 −1 −2 −3
f1 (ppm)

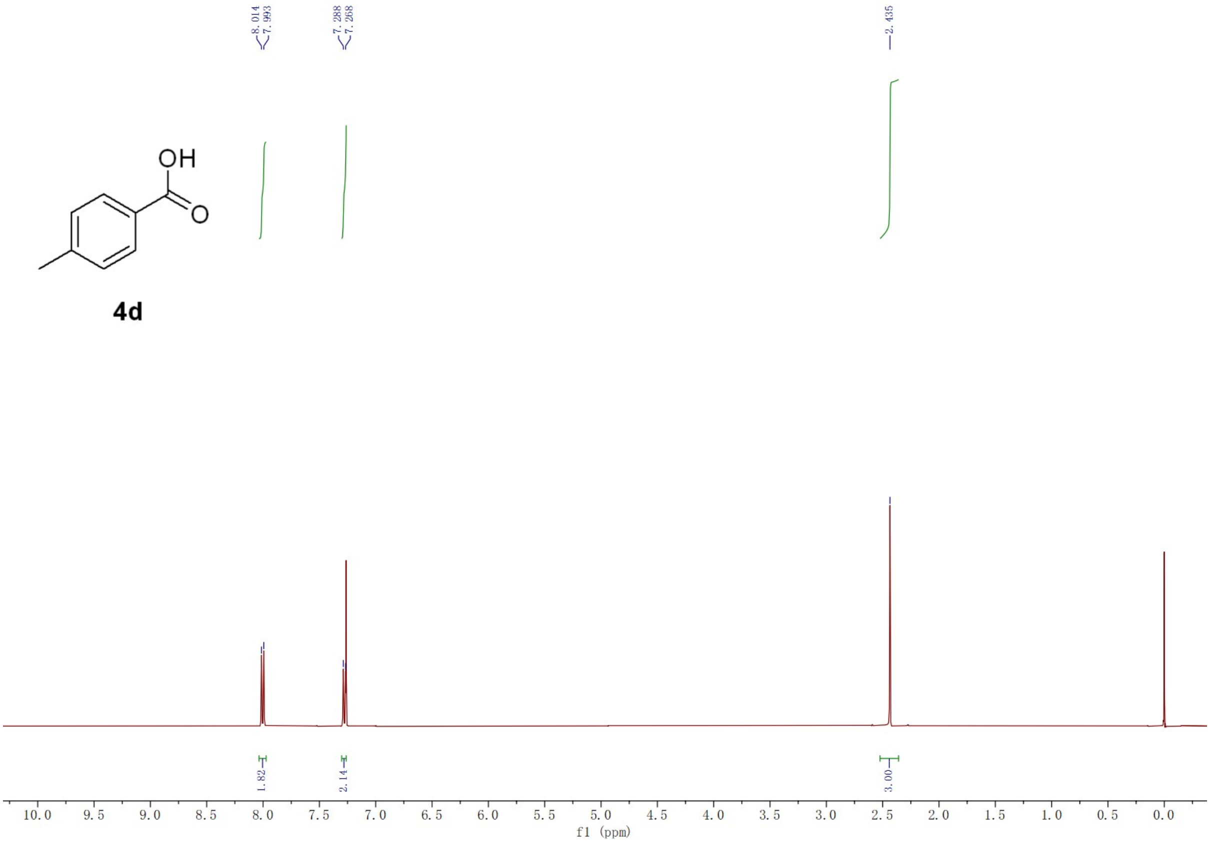

8.014
7.993
7.288
7.268
2.435
OH
O
4d
1.82
2.14
3.00
10.0 9.5 9.0 8.5 8.0 7.5 7.0 6.5 6.0 5.5 5.0 4.5 4.0 3.5 3.0 2.5 2.0 1.5 1.0 0.5 0.0
f1 (ppm)

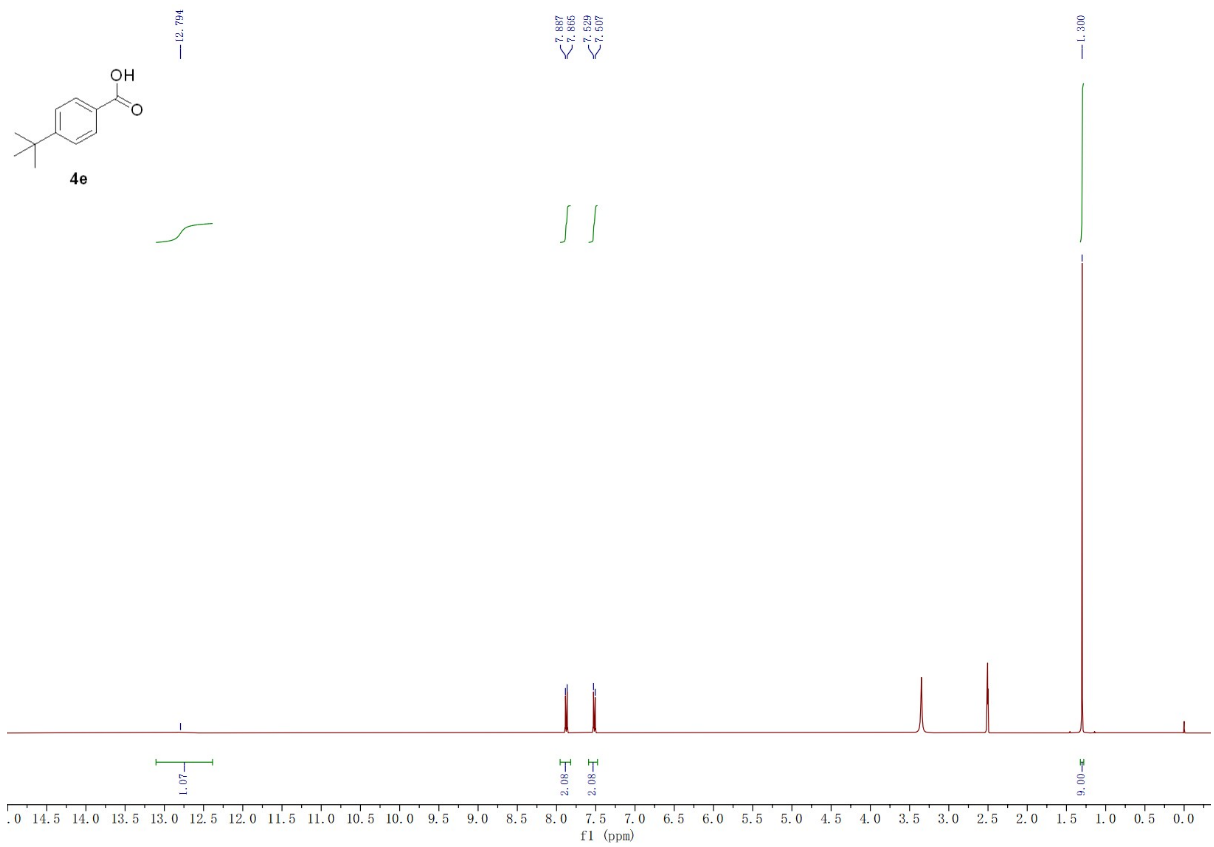
OH
O
4e
12.794
7.887
7.865
7.529
7.507
1.300
1.07
2.08
2.08
9.00
f1 (ppm)

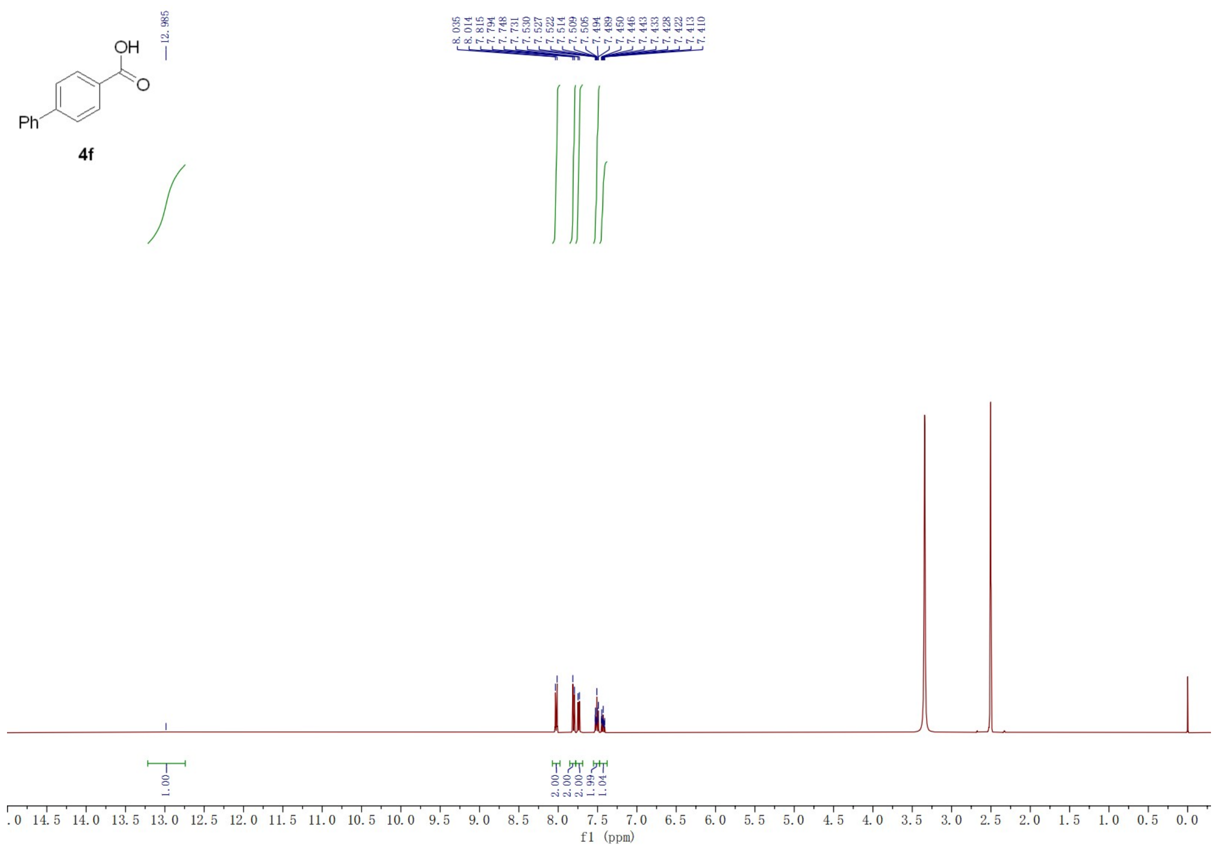
OH
O
Ph
4f
12.985
8.035
8.014
7.815
7.794
7.748
7.731
7.530
7.527
7.522
7.514
7.509
7.505
7.494
7.489
7.450
7.446
7.443
7.433
7.428
7.422
7.413
7.410
1.00
2.00
2.00
2.00
1.99
1.04
f1 (ppm)

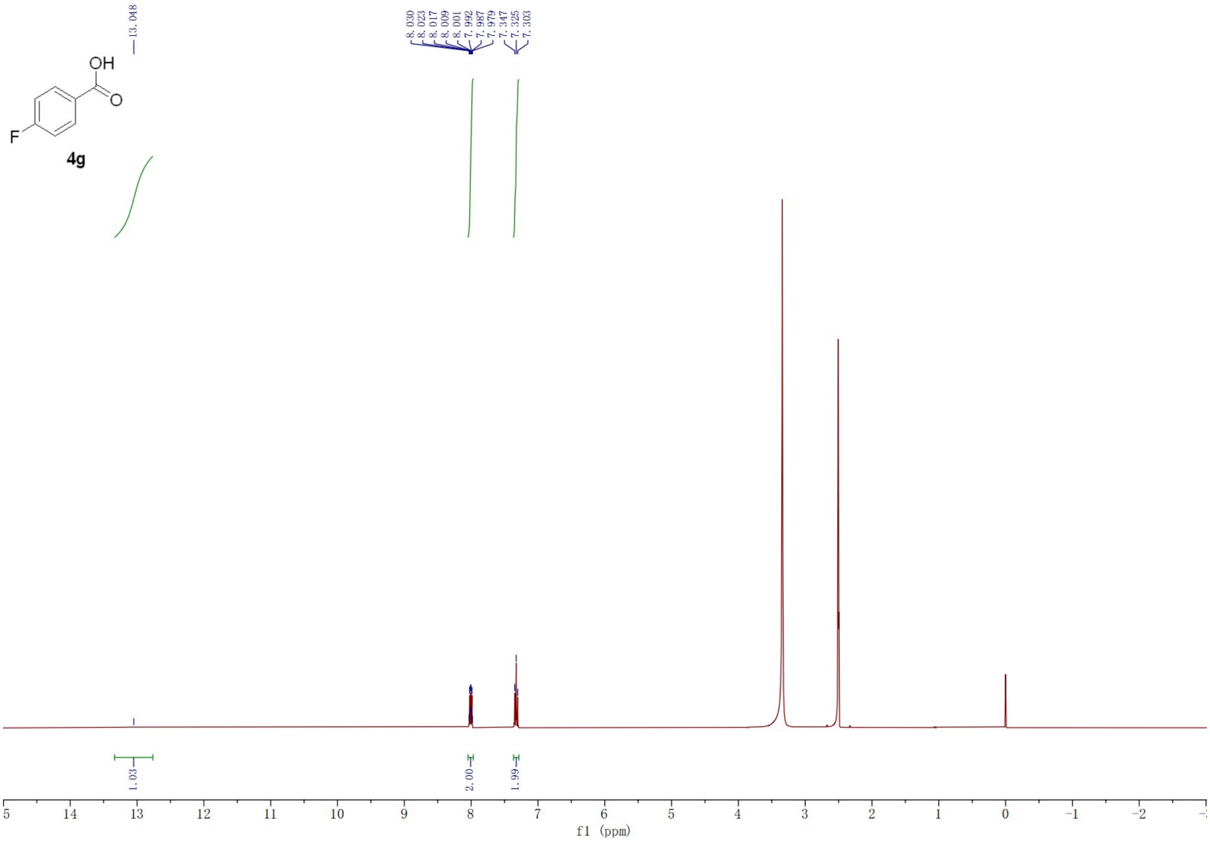
13.048
8.030
8.023
8.017
8.009
8.001
7.992
7.987
7.979
7.347
7.325
7.303
1.03
2.00
1.99
f1 (ppm)

4g

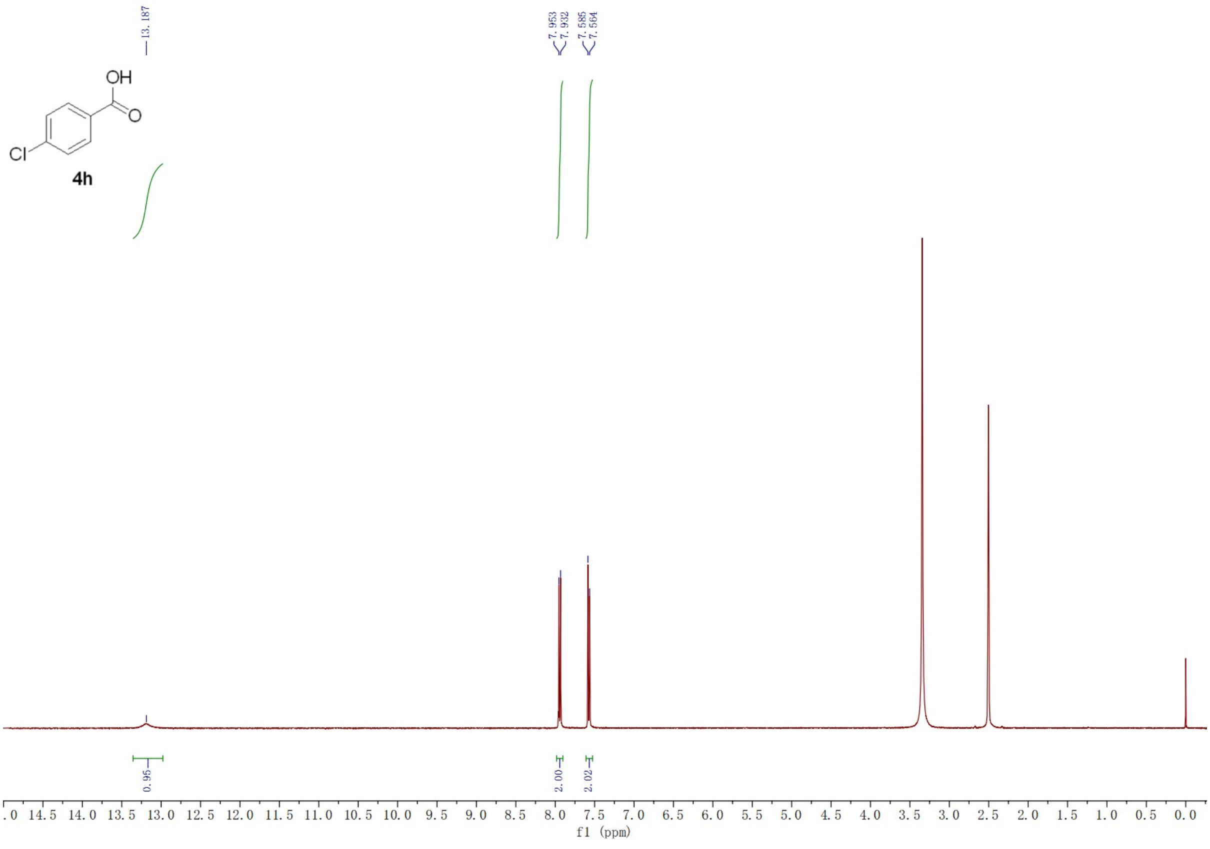
13.187
7.953
7.932
7.585
7.564
0.95
2.00
2.02
f1 (ppm)

4h

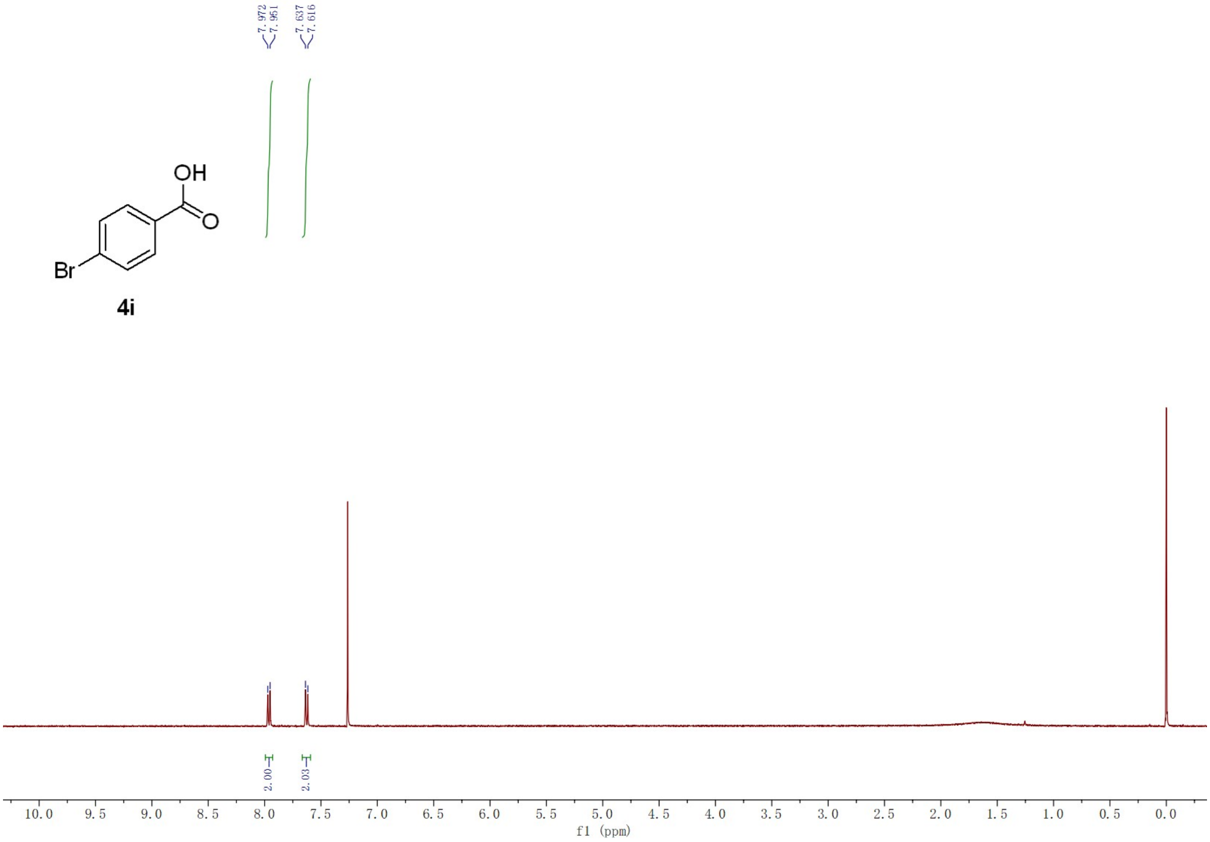
OH
O
Br
7.972
7.951
7.637
7.616
2.00
2.03
10.0 9.5 9.0 8.5 8.0 7.5 7.0 6.5 6.0 5.5 5.0 4.5 4.0 3.5 3.0 2.5 2.0 1.5 1.0 0.5 0.0
f1 (ppm)

4i

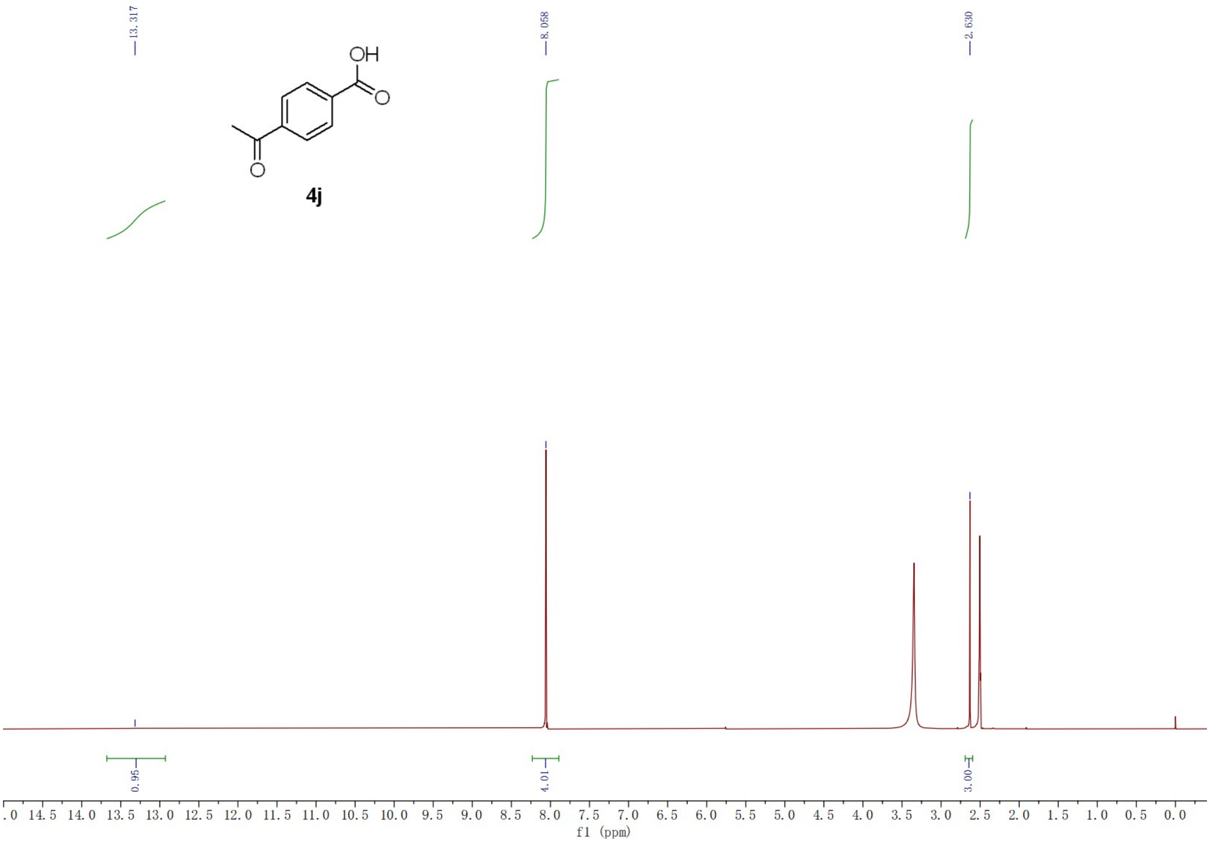
OH
O
O
13.317
8.058
2.630
0.95
4.01
3.00
.0 14.5 14.0 13.5 13.0 12.5 12.0 11.5 11.0 10.5 10.0 9.5 9.0 8.5 8.0 7.5 7.0 6.5 6.0 5.5 5.0 4.5 4.0 3.5 3.0 2.5 2.0 1.5 1.0 0.5 0.0
f1 (ppm)

4j

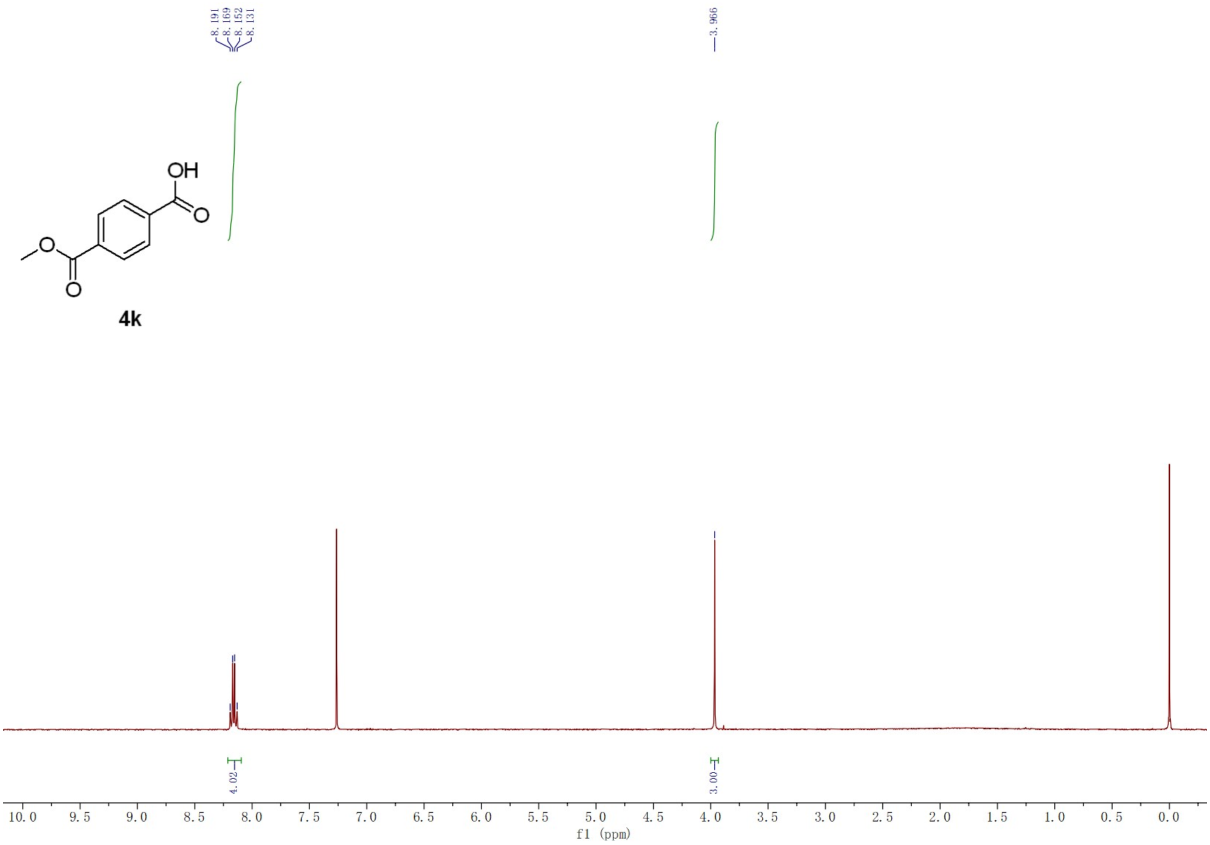
8.191
8.169
8.152
8.131
3.966
OH
O
O
O
4k
4.02
3.00
10.0 9.5 9.0 8.5 8.0 7.5 7.0 6.5 6.0 5.5 5.0 4.5 4.0 3.5 3.0 2.5 2.0 1.5 1.0 0.5 0.0
f1 (ppm)

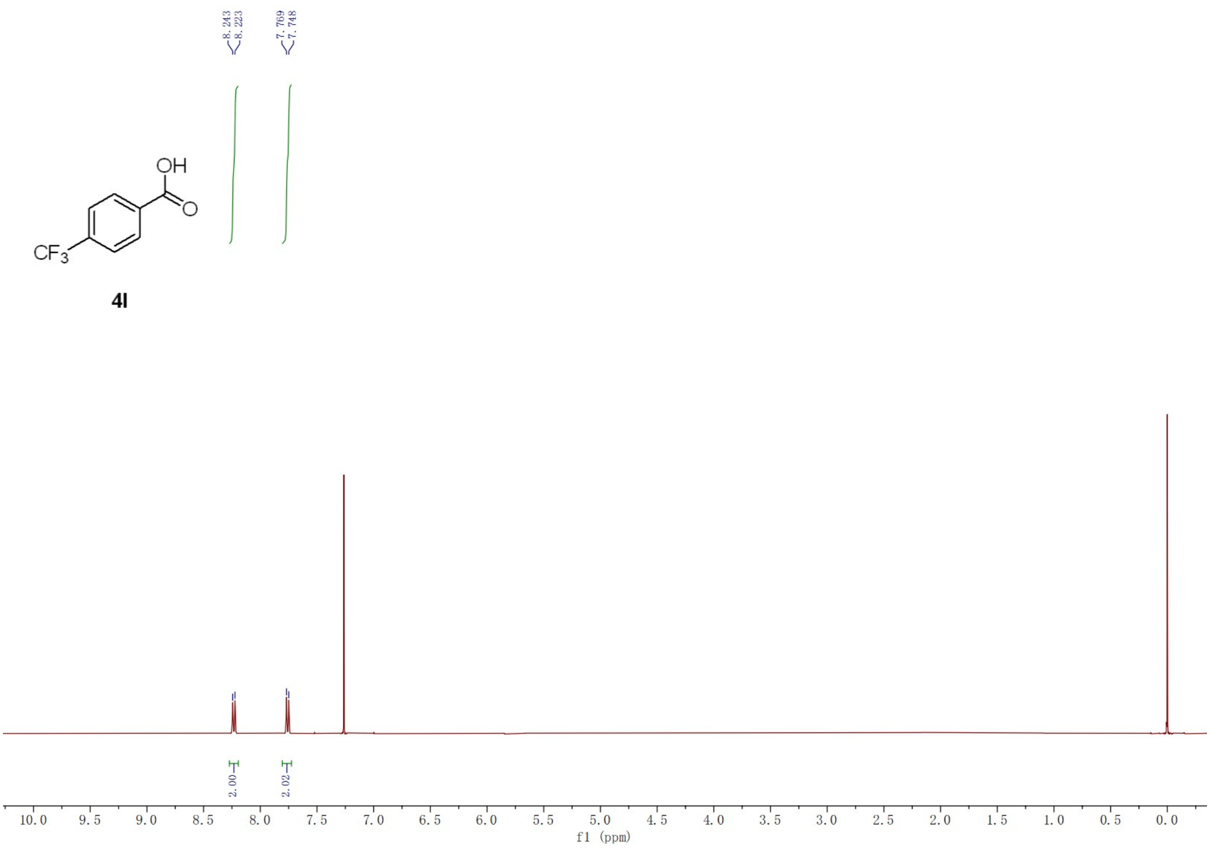
8.243
8.223
7.769
7.748
OH
O
CF_3
4l
2.00
2.02
10.0 9.5 9.0 8.5 8.0 7.5 7.0 6.5 6.0 5.5 5.0 4.5 4.0 3.5 3.0 2.5 2.0 1.5 1.0 0.5 0.0
f1 (ppm)

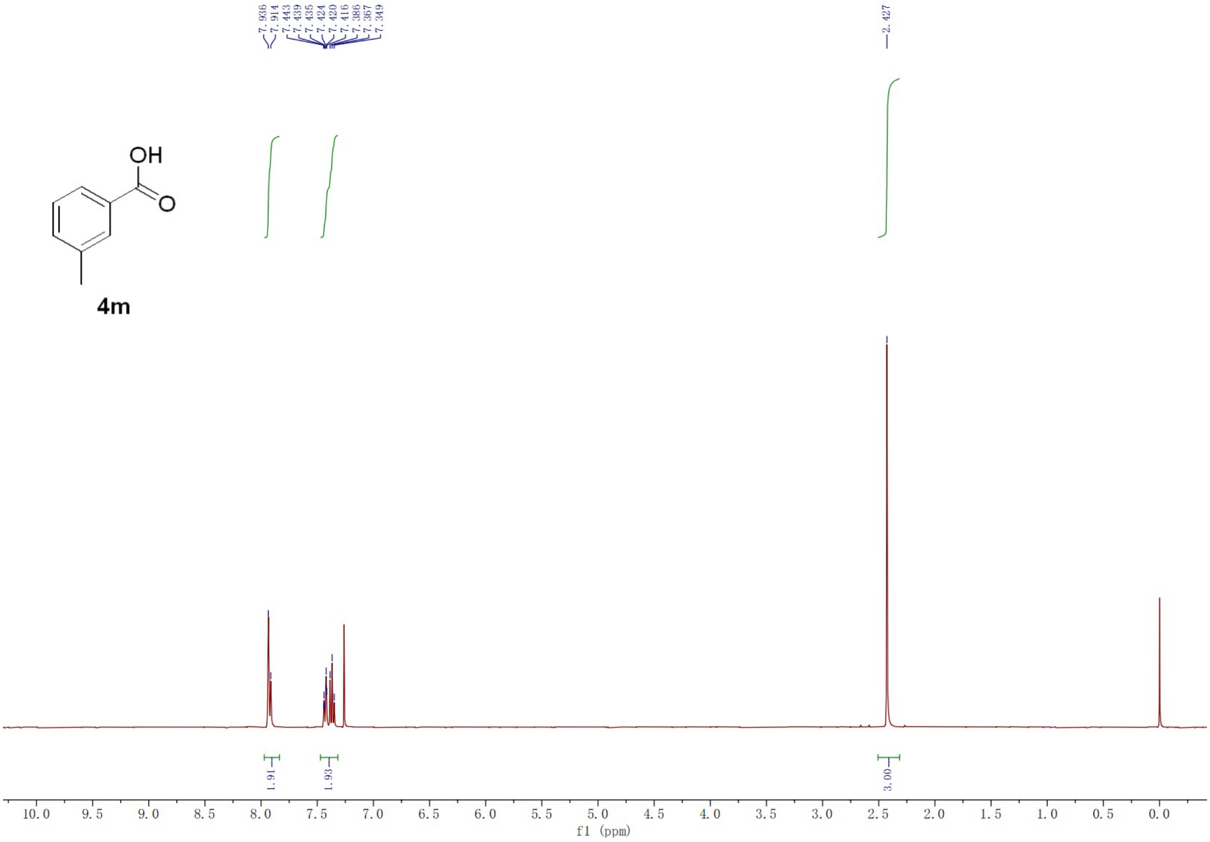
7.936
7.914
7.443
7.439
7.435
7.424
7.420
7.416
7.386
7.367
7.349
2.427
OH
O
1.91
1.93
3.00
10.0 9.5 9.0 8.5 8.0 7.5 7.0 6.5 6.0 5.5 5.0 4.5 4.0 3.5 3.0 2.5 2.0 1.5 1.0 0.5 0.0
f1 (ppm)

4m

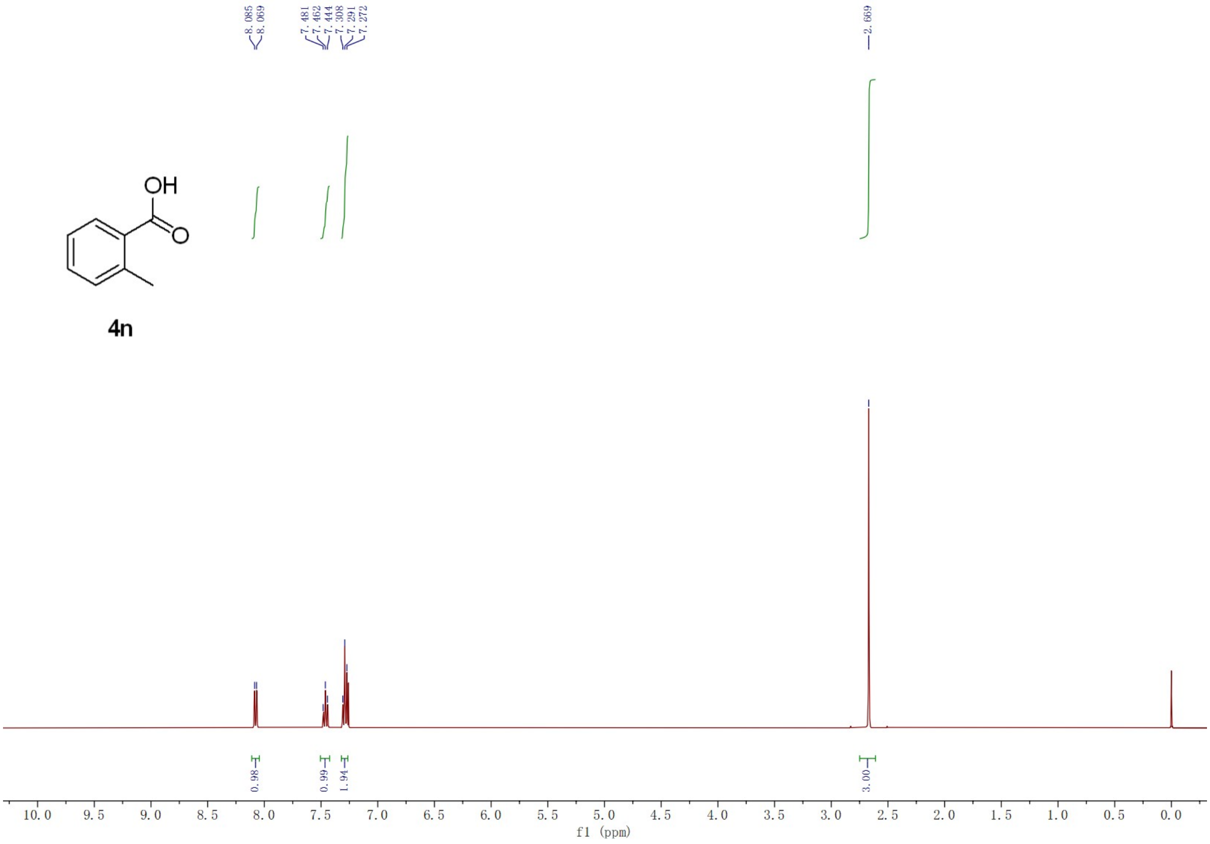
8.085
8.069
7.481
7.462
7.444
7.308
7.291
7.272
2.669
OH
O
0.98
0.99
1.94
3.00
10.0 9.5 9.0 8.5 8.0 7.5 7.0 6.5 6.0 5.5 5.0 4.5 4.0 3.5 3.0 2.5 2.0 1.5 1.0 0.5 0.0
f1 (ppm)

4n

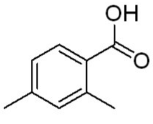
OH
O

4o

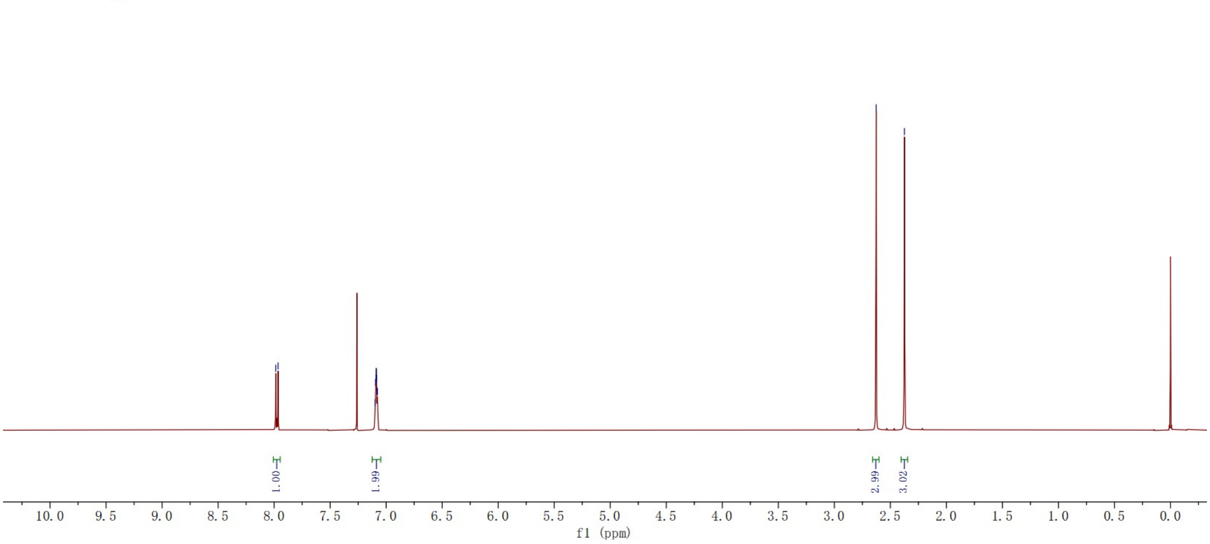
7.985
7.964
7.099
7.095
7.091
7.089
7.087
7.085
7.083
7.078
2.627
2.374
1.00
1.99
2.99
3.02
10.0
9.5
9.0
8.5
8.0
7.5
7.0
6.5
6.0
5.5
5.0
4.5
4.0
3.5
3.0
2.5
2.0
1.5
1.0
0.5
0.0
f1 (ppm)